NASA Contractor Report 189667
ICASE Report No. 92–26

ICASE

CROSSFLOW EFFECTS ON THE GROWTH RATE OF INVISCID GÖRTLER VORTICES IN A HYPERSONIC BOUNDARY LAYER

Yibin Fu
Philip Hall

Contract No. NAS1–18605
June 1992

Institute for Computer Applications in Science and Engineering
NASA Langley Research Center
Hampton, Virginia 23665–5225

Operated by the Universities Space Research Association

National Aeronautics and
Space Administration

Langley Research Center
Hampton, Virginia 23665-5225

CROSSFLOW EFFECTS ON THE GROWTH RATE OF INVISCID GÖRTLER VORTICES IN A HYPERSONIC BOUNDARY LAYER

Yibin Fu and Philip Hall*
Department of Mathematics
University of Manchester
Manchester M13 9PL
UNITED KINGDOM

ABSTRACT

The effects of crossflow on the growth rate of inviscid Görtler vortices in a hypersonic boundary layer with pressure gradient are studied in this paper. Attention is focussed on the inviscid mode trapped in the temperature adjustment layer; this mode has greater growth rate than any other mode. The eigenvalue problem which governs the relationship between the growth rate, the crossflow amplitude and the wavenumber is solved numerically, and the results are then used to clarify the effects of crossflow on the growth rate of inviscid Görtler vortices. It is shown that crossflow effects on Görtler vortices are fundamentally different for incompressible and hypersonic flows. The neutral mode eigenvalue problem is found to have an exact solution, and as a by-product, we have also found the exact solution to a neutral mode eigenvalue problem which was formulated, but unsolved before, by Bassom and Hall (1991).

*This research was supported in part by the National Aeronautics and Space Administration under NASA Contract No. NAS1-18605 while the second author was in residence at the Institute for Computer Applications in Science and Engineering (ICASE), NASA Langley Research Center, Hampton, VA 23665. This work was also partially supported by NASA under Grant NASA 18107 and by USAF under Grant AFOSR89-0042.

1 Introduction

This paper continues our studies on the Görtler instability mechanism in hypersonic boundary layers. For a discussion of the motivation for such studies and background information, the reader is referred to our previous papers, Hall and Fu (1989) and Fu, Hall and Blackaby (1992). Both are concerned with linear stability properties of Görtler vortices, but the first studies a Chapman's law fluid and the second is devoted to a Sutherland's law fluid. A common feature between the results for these two types of fluids is that the most rapidly growing Görtler vortices in a hypersonic boundary layer are those trapped in the temperature adjustment layer sitting at the edge of the boundary layer over which the basic state temperature decays from its $O(M^2)$ values near the wall to its free stream value, here M is the free stream Mach number. The major differences when these two different viscosity laws are used are as follows. Firstly, using Chapman's viscosity law predicts an $O(M^2)$ Görtler number, whilst using Sutherland's viscosity law predicts a smaller $O(M^{3/2})$ Görtler number. Secondly, the evolution of Görtler vortices in Chapman fluids is less strongly affected by nonparallel effects than those in Sutherland fluids. This is due to the fact that when Chapman's law is used, the temperature adjustment layer is logarithmically thin whilst when Sutherland's law is used, the adjustment layer is much thicker. Certainly, for a hypersonic boundary layer across which the temperature varies significantly, it is more appropriate to use Sutherland's law to model the viscosity of the fluids. Thus, in our later papers, Fu and Hall (1992a, 1992b) which study nonlinear development and secondary instabilities, Sutherland's viscosity law has been consistently used. In Fu and Hall (1992a), we have shown how Görtler vortices may grow in the neighbourhood of the neutrally stable position to form a large amplitude vortex structure which consists of a core region bounded by two viscous transition layers. Once such a structure has been established, various secondary instabilities in the form of traveling waves may be triggered off. There are at least two such secondary instabilities which have been observed in experiments. The first is called the wavy vortex mode of instability which makes the vortex boundaries wavy and which is located in the two viscous transition layers. This secondary instability has been studied in Fu and Hall (1992a). The other type is an inviscid instability which can exist because of the inflexional nature of the steady state. In Fu and Hall (1992b), we have shown how the change in the basic flow caused by the large mean flow correction of Görtler vortices would affect the growth rate of Rayleigh instability.

All of our previous studies in the hypersonic context have been concerned with problems which arise when Görtler vortices occur in two-dimensional boundary layers, but in many practical situations, the basic boundary layer may be three-dimensional. Boundary layer flows over a three-dimensional obstacle or over a turbine blade are such examples. A more

significant example is the boundary layer flow over the two areas of concave curvature on the lower side of a modern laminar flow airfoil which is fully three-dimensional when the wing is swept. Obviously, in order to effectively control or delay transition, the role played by a crossflow component in the basic flow should be fully understood.

This paper may be considered as extending the Hall (1985) and Bassom and Hall (1991) studies on crossflow effects in incompressible flows to hypersonic flows. It is also related to the recent work by Dando (1992) on crossflow effects in compressible flows. All of these studies have shown that crossflow has a stabilizing effect on Görtler vortices, and more importantly, Görtler vortices may be completely stabilized by the three-dimensional nature of the basic state. One objective of the present paper is to give a quantitative description of the stabilizing effect of a crossflow on Görtler vortices in hypersonic boundary layers.

As has been observed before by Hall (1985) for incompressible flows, the case when the crossflow velocity component is a constant multiplier of the streamwise velocity component is degenerate in the sense that by a suitable transformation, the problem can be reduced to a Görtler problem corresponding to a two-dimensional basic state. This degeneracy happens when there is no pressure gradient in the inviscid flow. Thus in order to reveal the genuine implications of having a crossflow, we avoid this degeneracy by assuming in this paper that there exists a pressure gradient in the inviscid flow. However, as has been shown by Stewartson (1964), when there is a pressure gradient in the boundary layer, analytical solutions to the boundary layer equations are possible only if we make three assumptions, one of which is that the viscosity should be given by Chapman's law. In order to make the necessary analytical progress, we shall assume that this is the case. Thus the present paper is more relevant to Hall and Fu (1989).

An important property of a hypersonic boundary layer is that the chordwise acceleration of a fixed fluid particle in the basic state is asymptotically large and in the opposite direction to the centrifugal acceleration due to the curvature of the wall. This negative chordwise acceleration has been interpreted in our previous papers as effectively producing a negative curvature (or equivalently a negative Görtler number). Thus the curvature of the wall should be large enough to overcome this negative curvature due to the basic state if Görtler vortices are to exist at all. In this paper, we assume that the Görtler number is of the same order as that of the effective negative Görtler number due to the basic state curvature. Then the large resultant Görtler number drives a large growth rate and as a result, the eigenvalue problem determining the growth rate is essentially inviscid. The main aim of this paper is to determine how the existence of a crossflow would modify the growth rate of these inviscid Görtler vortices.

The rest of this paper is organized as follows. As a preparation to later analysis, we first

discuss in the next section the solutions to the three-dimensional basic state when there is a pressure gradient. In section 3 we formulate the general linear Görtler instability problem which is then specialized in section 4 to the inviscid problem mentioned above. Sections 4 and 5 are devoted to the non-neutral and neutral solutions respectively, and in the final section we discuss our results and make some conclusions.

2 The basic state

Consider a hypersonic boundary layer over a rigid wall of variable curvature $(1/A)\kappa(x^*/L)$, where L is a typical streamwise length scale and A is a lengthscale characterizing the radius of curvature of the wall. We choose a curvilinear coordinate system (x^*, y^*, z^*) with x^* measuring distance along the wall, y^* perpendicular to the wall and z^* in the spanwise direction. To fix ideas, we may assume that the rigid wall is the surface of an infinite cylinder; the z-axis is then aligned with a generator of the cylinder (see Fig.1). The velocity components are denoted by (u^*, v^*, w^*) and density, temperature and viscosity by ρ^*, T^* and μ^* respectively. The free stream values of these quantities will be signified by a subscript ∞. The Reynolds number R, the curvature parameter $\triangle$ and the Görtler number G are defined by

$$R = \frac{u^*_\infty L \rho^*_\infty}{\mu^*_\infty}, \quad \triangle = \frac{L}{A}, \quad G = 2R^{1/2}\triangle . \tag{2.1}$$

We assume that the Reynolds number is large, while $\triangle$ is taken to be small. In the context of incompressible flows, the characteristic values of G for instability are $O(1)$; whilst in hypersonic flows G is $O(M^2)$ when Chapman's viscosity law is used (see Hall and Fu (1989)), and is $O(M^{3/2})$ when Sutherland's viscosity law is used (see Fu, Hall and Blackaby (1992)). In the following analysis, coordinates (x^*, y^*, z^*) are scaled on $(L, R^{-1/2}L, R^{-1/2}L)$, the velocity (u^*, v^*, w^*) is scaled on $(u^*_\infty, R^{-1/2}u^*_\infty, R^{-1/2}u^*_\infty)$ and other quantities such as ρ^*, T^*, and μ^* are scaled on their free stream values with the only exception that the pressure p^* is scaled on $\rho^*_\infty u^{*2}_\infty$ and the bulk viscosity λ^* is scaled on μ^*_∞. All dimensionless quantities will be denoted by the same letters without a superscript $*$. For an ideal gas without dissociation, the continuity, Navier-Stokes, energy equations and the equation of state are, to leading order, given by

$$\frac{\partial \rho}{\partial t} + \frac{\partial}{\partial x_\beta}(\rho v_\beta) = 0, \tag{2.2}$$

$$\rho \frac{Du}{Dt} = -\frac{\partial p}{\partial x} + \frac{\partial}{\partial y}(\mu \frac{\partial u}{\partial y}) + \frac{\partial}{\partial z}(\mu \frac{\partial u}{\partial z}), \tag{2.3}$$

$$\rho(\frac{Dv}{Dt} + \frac{1}{2}G\kappa u^2) = -R\frac{\partial p}{\partial y} + \frac{\partial}{\partial y}\left\{(\lambda - \frac{2}{3}\mu)\frac{\partial v_\beta}{\partial x_\beta}\right\} + \frac{\partial}{\partial x_\beta}(\mu \frac{\partial v_\beta}{\partial y})$$

$$+\frac{\partial}{\partial y}(\mu\frac{\partial v}{\partial y})+\frac{\partial}{\partial z}(\mu\frac{\partial v}{\partial z}), \tag{2.4}$$

$$\rho\frac{Dw}{Dt}=-R\frac{\partial p}{\partial z}+\frac{\partial}{\partial z}\left\{(\lambda-\frac{2}{3}\mu)\frac{\partial v_\beta}{\partial x_\beta}\right\}+\frac{\partial}{\partial x_\beta}(\mu\frac{\partial v_\beta}{\partial z})$$
$$+\frac{\partial}{\partial y}(\mu\frac{\partial w}{\partial y})+\frac{\partial}{\partial z}(\mu\frac{\partial w}{\partial z}), \tag{2.5}$$

$$\rho\frac{DT}{Dt}=\mu(\gamma-1)M^2[(\frac{\partial u}{\partial y})^2+(\frac{\partial u}{\partial z})^2]+(\gamma-1)M^2\frac{Dp}{Dt}$$
$$+\frac{1}{\sigma}\frac{\partial}{\partial y}(\mu\frac{\partial T}{\partial y})+\frac{1}{\sigma}\frac{\partial}{\partial z}(\mu\frac{\partial T}{\partial z}), \tag{2.6}$$

$$\gamma M^2 p=\rho T. \tag{2.7}$$

Here terms of relative order R^{-1} have been neglected and we have used a mixed notation in which (v_1,v_2,v_3) is identified with (u,v,w) and (x_1,x_2,x_3) with (x,y,z). Repeated suffices β signify summation from 1 to 3. The constants γ, M and σ are in turn the ratio of specific heats, the free stream Mach number and the Prandtl number defined by

$$\gamma=\frac{c_{p\infty}}{c_{v\infty}},\quad M^2=\frac{u_\infty^{*2}}{\gamma\bar{\Re}T_\infty^*}=\frac{u_\infty^{*2}}{a_\infty^2},\quad \sigma=\frac{\mu_\infty c_{p\infty}}{k_\infty},$$

where $\bar{\Re}$ is the gas constant, k is the coefficient of heat conduction, and $a_\infty=\sqrt{\gamma\bar{\Re}T_\infty^*}$ is the speed of sound in the free stream. In equations (2.3)–(2.6), the operator D/Dt is the material derivative and is given by

$$\frac{D}{Dt}=u\frac{\partial}{\partial x}+v\frac{\partial}{\partial y}+w\frac{\partial}{\partial z}.$$

The basic state is given by

$$(u,\ v,\ w)=(\bar{u}(x,y),\ \bar{v}(x,y),\ \bar{w}(x,y)),\quad T=\bar{T}(x,y),$$

$$\rho=\bar{\rho}(x,y),\quad \mu=\bar{\mu}(x,y), \tag{2.8}$$

where we have allowed for a non-zero crossflow component $\bar{w}(x,y)$. Such a three-dimensional boundary layer may easily be obtained if, for example, the angle of yaw of the cylinder Λ shown in Fig.1 is non-zero.

By substituting (2.8) into the governing equations (2.2)–(2.7), we find that the basic state satisfies

$$\frac{\partial}{\partial x}(\bar{\rho}\bar{u})+\frac{\partial}{\partial y}(\bar{\rho}\bar{v})=0, \tag{2.9}$$

$$\bar{\rho}\left(\bar{u}\frac{\partial\bar{u}}{\partial x}+\bar{v}\frac{\partial\bar{u}}{\partial y}\right)=-\frac{dP_1}{dx}+\frac{\partial}{\partial y}\left(\bar{\mu}\frac{\partial\bar{u}}{\partial y}\right), \tag{2.10}$$

$$\bar{\rho}\left(\bar{u}\frac{\partial\bar{w}}{\partial x}+\bar{v}\frac{\partial\bar{w}}{\partial y}\right)=\frac{\partial}{\partial y}\left(\bar{\mu}\frac{\partial\bar{w}}{\partial y}\right), \tag{2.11}$$

$$\bar{\rho}\left(\bar{u}\frac{\partial\bar{T}}{\partial x}+\bar{v}\frac{\partial\bar{T}}{\partial y}\right)-(\gamma-1)M^2\frac{dP_1}{dx}\bar{u}$$

$$=\frac{1}{\sigma}\frac{\partial}{\partial y}\left(\bar{\mu}\frac{\partial\bar{T}}{\partial y}\right)+\bar{\mu}(\gamma-1)M^2\left(\frac{\partial\bar{u}}{\partial y}\right)^2, \tag{2.12}$$

$$\gamma M^2 P_1=\bar{\rho}\bar{T}, \tag{2.13}$$

where P_1 is the inviscid solution for the pressure evaluated at $y=0$. The equation obtained from the y-momentum equation (2.4) is simply $\partial\bar{p}/\partial y=0$ which implies that $\bar{p}=\bar{p}(x)=P_1$. From the inviscid theory, we have the relation

$$\frac{dP_1}{dx}=-\rho_1 U_1\frac{dU_1}{dx}, \tag{2.14}$$

where ρ_1 and U_1 have the same meaning as P_1. If we introduce T_1, the inviscid solution for the temperature evaluated at $y=0$, then equation (2.13) can also be written as

$$\bar{\rho}\bar{T}=\rho_1 T_1. \tag{2.15}$$

In this paper, we assume that $dP_1/dx\neq 0$, i.e. there exists a pressure gradient in the inviscid flow. If $dP_1/dx=0$, then (2.10) and (2.11) together with the boundary conditions imply that $\bar{w}$ is a constant multiplier of $\bar{u}$, in which case the original three-dimensional basic state can be made two-dimensional by rotating the coordinate system about the y-axis by an angle given by $\tan^{-1}(\bar{w}/\bar{u})$, see Hall (1985).

We now turn to the solution of the basic state equations. The reader is referred to the book by Stewartson (1964) for a detailed discussion of these equations. Here we shall just give an outline of the necessary procedures and the main results.

The immediate consequence of including a pressure gradient is that similarity solutions are now only possible if we use Chapman's viscosity law

$$\mu=C(x)T, \tag{2.16}$$

assume that $\sigma=1$ and make the homenergic assumption. (We recall that analytical similarity solutions are possible without making any of the above assumptions if there is no pressure gradient). In this paper, we shall adopt these assumptions to make the necessary analytical progress. Then the first step in the solution is to determine the temperature $\bar{T}$ explicitly. To this end, we first eliminate dP_1/dx from (2.10) and (2.12) to obtain the following equation:

$$\bar{\rho}\left(\bar{u}\frac{\partial I}{\partial x}+\bar{v}\frac{\partial I}{\partial y}\right)=\frac{\partial}{\partial y}\left(\bar{\mu}\frac{\partial I}{\partial y}\right), \tag{2.17}$$

where

$$I = \bar{T} + \frac{1}{2}(\gamma - 1)M^2\bar{u}^2. \tag{2.18}$$

On comparing (2.17) with (2.11), we deduce that the general solution to (2.17) can be written as

$$I = -A\bar{w} + const.,$$

where A is an arbitrary constant to be fixed by boundary conditions. Hence

$$\bar{T} + \frac{1}{2}(\gamma - 1)M^2\bar{u}^2 + A\bar{w} = const.$$

$$= T_1 + \frac{1}{2}(\gamma - 1)M^2U_1^2 + AW_1, \tag{2.19}$$

where W_1 is the inviscid crossflow velocity component evaluated at $y = 0$ and is given by

$$W_1 = \frac{U_\infty \sin\Lambda}{R^{-1/2}u_\infty^*} = R^{1/2}\tan\Lambda,$$

since $u_\infty^* = U_\infty \cos\Lambda$ (see Fig.1) and W_1 has been scaled on $R^{-1/2}u_\infty^*$. Guided by previous results for incompressible flows, we assume that the yaw angle Λ is of order $R^{-1/2}$ (this is the order at which crossflow begins to affect the growth of Görtler vortices), so that W_1 is an order one constant under the large Reynolds number limit. We see that the the size of W_1 can be adjusted by varying Λ.

By the homenergic assumption, the total energy (scaled by c_pT_∞) in the inviscid flow is a constant and so

$$T_1 + \frac{1}{2}(\gamma - 1)M^2U_1^2 = 1 + \frac{1}{2}(\gamma - 1)M^2, \tag{2.20}$$

where the left and right hand sides are the scaled energy evaluated at $y = 0$ and $y = \infty$, respectively. With the use of (2.20), (2.19) can be written as

$$\bar{T} + \frac{1}{2}(\gamma - 1)M^2\bar{u}^2 + A(\bar{w} - W_1) = 1 + \frac{1}{2}(\gamma - 1)M^2. \tag{2.21}$$

If we denote the temperature at the wall by T_w, then (2.21) together with $\bar{u}(0) = \bar{w}(0) = 0$ implies that

$$A = \frac{T_w - 1 - \frac{1}{2}(\gamma - 1)M^2}{W_1}, \tag{2.22}$$

and so (2.21) becomes

$$\bar{T} = 1 + \frac{1}{2}(\gamma - 1)M^2(1 - \bar{u}^2) + (1 - \frac{\bar{w}}{W_1})\left\{T_w - 1 - \frac{1}{2}(\gamma - 1)M^2\right\}. \tag{2.23}$$

In the special case when the wall is insulated ($\partial\bar{T}/\partial y = 0$ at $y = 0$), it is easy to show with the aid of (2.23) that the wall temperature must necessarily be given by

$$T_w|_{\text{wall insulated}} = 1 + \frac{1}{2}(\gamma - 1)M^2 \stackrel{\text{def.}}{=} T_r, \tag{2.24}$$

where T_r is usually referred to as the recovery temperature. Once we know the expression for $\bar{T}$, we can now solve (2.9)−(2.13) by introducing a variable $\bar{Y}$ by

$$\bar{Y} = \int_0^y \bar{\rho} dy \tag{2.25}$$

and expressing $\bar{u}$ and $\bar{v}$ in terms of a function $\psi(x, \bar{Y})$ as

$$\bar{u} = \frac{\partial \psi}{\partial \bar{Y}}, \quad \bar{v} = -\frac{1}{\bar{\rho}}(\frac{\partial \psi}{\partial x} + \bar{u}\bar{Y}_x). \tag{2.26}$$

Then the continuity equation (2.9) is satisfied and (2.10), (2.11) become

$$\frac{\partial \psi}{\partial \bar{Y}} \frac{\partial^2 \psi}{\partial x \partial \bar{Y}} - \frac{\partial \psi}{\partial x} \frac{\partial^2 \psi}{\partial \bar{Y}^2} = -\frac{\bar{T}}{\gamma M^2 P_1} \frac{dP_1}{dx} + C(x)\gamma M^2 P_1 \frac{\partial^3 \psi}{\partial \bar{Y}^3}, \tag{2.27}$$

$$\frac{\partial \psi}{\partial \bar{Y}} \frac{\partial \bar{w}}{\partial x} - \frac{\partial \psi}{\partial x} \frac{\partial \bar{w}}{\partial \bar{Y}} = C(x)\gamma M^2 P_1 \frac{\partial^2 \bar{w}}{\partial \bar{Y}^2}. \tag{2.28}$$

Before we could look for similarity solutions for the above equations, we have to eliminate the appearance of $\bar{u}$ through $\bar{T}$ on the right hand side of (2.27). This can be achieved by introducing two new variable (X, Y) through

$$X = \int^x \gamma M^2 P_1(x) \sqrt{T_1(x)} C(x) dx, \quad Y = \sqrt{T_1(x)} \bar{Y}. \tag{2.29}$$

In terms of X and Y, equations (2.27) and (2.28) can be written as

$$\frac{\partial \psi}{\partial Y} \frac{\partial^2 \psi}{\partial X \partial Y} - \frac{\partial \psi}{\partial X} \frac{\partial^2 \psi}{\partial Y^2} = \frac{\partial^3 \psi}{\partial Y^3} + V_1 \frac{dV_1}{dX} \left\{ 1 + (1 - \frac{\bar{w}}{W_1})(\frac{T_w}{T_r} - 1) \right\}, \tag{2.30}$$

$$\frac{\partial \psi}{\partial Y} \frac{\partial \bar{w}}{\partial X} - \frac{\partial \psi}{\partial X} \frac{\partial \bar{w}}{\partial Y} = \frac{\partial^2 \bar{w}}{\partial Y^2}, \tag{2.31}$$

after (2.15), (2.13), (2.14) and (2.20) have been used. Here

$$V_1(X) = \frac{U_1}{\sqrt{T_1}}. \tag{2.32}$$

Equations (2.30) and (2.31) are to be solved subject to the following boundary conditions:

$$\psi = \frac{\partial \psi}{\partial y} = 0, \quad \bar{w} = 0 \quad \text{at } Y = 0,$$

$$\frac{\partial \psi}{\partial y} \to V_1, \quad \bar{w} \to W_1 \quad \text{as } Y \to \infty. \tag{2.33}$$

The above boundary value problem admits similarity solutions of the form

$$\psi = a(X) f(\eta), \quad \bar{w} = W_1 g(\eta), \quad \eta = \frac{Y}{b(X)}, \tag{2.34}$$

if V_1 is of the form

$$V_1 = UX^m. \tag{2.35}$$

By substituting (2.34) and (2.35) into (2.30)–(2.33), it is easy to show that

$$a(X) = \sqrt{\frac{2U}{1+m}X^{1+m}}, \quad b(X) = \sqrt{\frac{2}{U(1+m)}X^{1-m}}, \tag{2.36}$$

and the boundary value problem then reduces to the following simpler form:

$$f''' + ff'' + \beta\left\{1 - f'^2 + (n-1)(1-g)\right\} = 0, \tag{2.37}$$

$$g'' + fg' = 0, \tag{2.38}$$

$$f(0) = f'(0) = g(0) = 0, \tag{2.39}$$

$$f'(\infty) = g(\infty) = 1, \tag{2.40}$$

where the constant β and the cooling coefficient n in (2.37) are given by

$$\beta = \frac{2m}{1+m}, \qquad n = \frac{T_w}{T_r}. \tag{2.41}$$

On substituting (2.34a) into (2.26a), we obtain $\bar{u} = U_1 f'(\eta)$ and insertion of this expression and (2.34b) into (2.23) then yields the following expression for $\bar{T}$:

$$\bar{T} = T_1 f'^2 + [1 + \frac{1}{2}(\gamma - 1)M^2]\left\{1 - f'^2 + (n-1)(1-g)\right\}. \tag{2.42}$$

Our previous experience with the zero-pressure gradient problem shows that the stability properties of a hypersonic boundary layer depend very much on the properties of the basic state temperature distribution. When there is no pressure gradient, it is known from Hall and Fu (1989) that the boundary layer splits into two sublayers in the large Mach number limit: a wall layer where $\bar{T} = O(M^2)$ and a logarithmically thin temperature adjustment layer where $\bar{T} = O(1)$, and it is the latter sublayer which supports the most rapidly growing mode. In order to determine the precise boundary layer structure for the present non-zero pressure gradient problem, we first need to know the large η behaviour of f' and g. It can be shown from (2.37) and (2.38) that as $\eta \to \infty$,

$$f'(\eta) = 1 + \left\{\frac{(n-1)c_2}{2(\eta-\omega)} - \frac{c_1}{(\eta-\omega)^{1+2\beta}}\right\} e^{-\frac{1}{2}(\eta-\omega)^2} + \cdots,$$

$$g = 1 - \frac{c_2}{\eta-\omega} e^{-\frac{1}{2}(\eta-\omega)^2} + \cdots, \tag{2.43}$$

where ω, c_1 and c_2 are constants. On substituting (2.43) into (2.42), we find that as $\eta \to \infty$,

$$\bar{T} = T_1 + NM^2 e^{-\frac{1}{2}(\eta-\omega)^2} \cdot \frac{1}{(\eta-\omega)^{1+2\beta}} + \cdots, \tag{2.44}$$

where

$$N = c_1(\gamma - 1).$$

In order to determine the location and thickness of the temperature adjustment layer at which $\bar{T} = O(1)$, it is convenient to let

$$M^2 e^{-\frac{1}{2}(\eta-\omega)^2} \cdot \frac{1}{(\eta-\omega)^{1+2\beta}} = \frac{T_1}{N} e^{\tilde{y}}.$$

Solving this equation for $(\eta - \omega)$ gives

$$\eta - \omega = M_1 - \frac{\tilde{y} + (1+2\beta)\log M_1}{M_1}, \tag{2.45}$$

where

$$M_1 = \sqrt{2\log M^2}.$$

Equation (2.45) shows that the temperature adjustment layer is at $\eta = O(M_1)$ and is of $O(1/M_1)$ thickness. In the adjustment layer, $\bar{T}$ is given by

$$\bar{T} = T_1(1 + e^{\tilde{y}}), \tag{2.46}$$

so that $\bar{T} \to T_1$ as $\tilde{y} \to -\infty$ and matches with the wall layer solution (2.44) as $\tilde{y} \to +\infty$.

In summary, the basic state under consideration corresponds to $V_1 = U_1/\sqrt{T_1} = UX^m$ and has solution given by

$$\bar{u} = U_1 f'(\eta), \quad \bar{v} = -\frac{\bar{T}}{\rho_1 T_1}\left\{\rho_1 T_1^{3/2} C(x) a'(X) f(\eta) + U_1 f'(\eta)(\bar{Y}_x + \frac{T_1'}{2T_1^{3/2}} Y)\right\}, \tag{2.47}$$

$$\bar{w} = W_1 g(\eta), \quad \bar{T} = T_1 f'^2 + [1 + \frac{1}{2}(\gamma-1)M^2]\left\{1 - f'^2 + A_1(1-g)\right\}, \tag{2.48}$$

where the new variables $X, \bar{Y}, Y$ and η are related to (x, y) by

$$X = \int^x \gamma M^2 P_1(x)\sqrt{T_1(x)}C(x)dx, \quad Y = \sqrt{T_1(x)}\bar{Y}, \quad \bar{Y} = \int_0^y \bar{\rho} dy, \quad \eta = \frac{Y}{b(X)}, \tag{2.49}$$

and it can be shown that the function $\bar{Y}_x$ appearing in (2.47b) is given by

$$\bar{Y}_x = \frac{P_1'}{P_1\bar{T}}\int_0^{\bar{Y}} \bar{T}(x,\bar{Y})d\bar{Y} - \frac{1}{\bar{T}}\int_0^{\bar{Y}} \frac{\partial \bar{T}(x,\bar{Y})}{\partial x} d\bar{Y}. \tag{2.50}$$

In section 4, we shall need to know the asymptotic expressions for these basic state quantities and their various derivatives in the temperature adjustment layer in order to determine the relative orders of the perturbation quantities. These expressions are listed in the Appendix at the end of this paper.

3 The linear Görtler instability problem

In order to determine the evolutionary behaviour of Görtler vortices in the hypersonic boundary layer described above, we now superimpose a vortex structure on the basic state. Thus the total flow is written as

$$u = \bar{u} + U\mathrm{e}^{iaz}, \quad v = \bar{v} + V\mathrm{e}^{iaz}, \quad w = \bar{w} + W\mathrm{e}^{iaz},$$

$$p = P_1 + \frac{1}{R}P\mathrm{e}^{iaz}, \quad T = \bar{T} + \theta\mathrm{e}^{iaz}, \quad \rho = \bar{\rho} + \tilde{\rho}\mathrm{e}^{iaz}. \tag{3.1}$$

Here U, V, etc. are functions of X and Y only. On substituting (3.1) into the governing equations (2.9)–(2.13) and linearizing, we obtain the following perturbation equations:

$$\frac{\theta}{\bar{T}^2}L(\bar{T}) - \frac{\theta}{\bar{\rho}\bar{T}}L(\bar{\rho}) - \frac{\theta}{\bar{T}}(\bar{u}_x + \bar{v}_y) - \frac{1}{\bar{T}}(L(\theta) + ia\bar{w}\theta)$$

$$+ \frac{\partial U}{\partial x} + \frac{\partial V}{\partial y} + iaW + \frac{1}{\bar{\rho}}\left(U\frac{\partial\bar{\rho}}{\partial x} + V\frac{\partial\bar{\rho}}{\partial y}\right) = 0, \tag{3.2}$$

$$\bar{\rho}\{L(U) + ia\bar{w}U + U\bar{u}_x + V\bar{u}_y\} - \frac{\bar{\rho}}{\bar{T}}L(\bar{u})\theta$$

$$= \frac{\partial}{\partial y}\left(\bar{\mu}\frac{\partial U}{\partial y}\right) - a^2\bar{\mu}U + \frac{\partial}{\partial y}(\tilde{\mu}\bar{u}_y\theta), \tag{3.3}$$

$$(\bar{\rho}\bar{v}_x + \bar{\rho}G\kappa\bar{u})U + \frac{2}{3}\bar{\mu}_y\frac{\partial U}{\partial x} - \frac{\bar{\mu}}{3}\frac{\partial^2 U}{\partial x\partial y} - \bar{\mu}_x\frac{\partial U}{\partial y} - ia\cdot\frac{\bar{\mu}}{3}\frac{\partial W}{\partial y}$$

$$+ia\cdot\frac{2}{3}\bar{\mu}_y W + \bar{\rho}\{L(V) + ia\bar{w}V\} + \bar{\rho}\bar{v}_y V + a^2\bar{\mu}V - \frac{4}{3}\frac{\partial}{\partial y}\left(\bar{\mu}\frac{\partial V}{\partial y}\right)$$

$$+\frac{\partial P}{\partial y} - \tilde{\mu}\bar{u}_y\frac{\partial\theta}{\partial x} - ia\tilde{\mu}\bar{w}_y\theta + (\frac{2}{3}\tilde{\mu}\bar{u}_x - \frac{4}{3}\tilde{\mu}\bar{v}_y)\frac{\partial\theta}{\partial y}$$

$$- \left\{\frac{\bar{\rho}}{\bar{T}}[L(\bar{v}) + \frac{1}{2}G\kappa\bar{u}^2] - \frac{2}{3}(\tilde{\mu}\bar{u}_x)_y + \frac{4}{3}(\tilde{\mu}\bar{v}_y)_y + (\tilde{\mu}\bar{u}_y)_x\right\}\theta = 0, \tag{3.4}$$

$$ia\bar{\mu}_x U + ia\cdot\frac{\bar{\mu}}{3}\frac{\partial U}{\partial x} - \bar{\rho}\bar{w}_x U + ia\bar{\mu}_y V + ia\cdot\frac{\bar{\mu}}{3}\frac{\partial V}{\partial y} - \frac{4}{3}\bar{\mu}a^2 W$$

$$+\frac{\partial}{\partial y}\left(\bar{\mu}\frac{\partial W}{\partial y}\right) - \bar{\rho}\bar{w}_y V - iaP - ia\cdot\frac{2}{3}\tilde{\mu}(\bar{u}_x + \bar{v}_y)\theta + \tilde{\mu}\bar{w}_y\frac{\partial\theta}{\partial y}$$

$$+ [\frac{\tilde{\rho}}{\bar{T}}L(\bar{w}) + (\tilde{\mu}\bar{w}_y)_y]\theta - \bar{\rho}[L(W) + ia\bar{w}W] = 0, \tag{3.5}$$

$$[\bar{\rho}\bar{T}_x - (\gamma-1)M^2\frac{dP_1}{dx}]U - 2(\gamma-1)M^2\cdot\bar{\mu}\bar{u}_y\frac{\partial U}{\partial y} + \bar{\rho}\bar{T}_y V$$

$$+\bar{\rho}[L(\theta) + ia\bar{w}\theta] + a^2\cdot\frac{\bar{\mu}}{\sigma}\theta - \frac{1}{\sigma}\frac{\partial}{\partial y}\left(\bar{\mu}\frac{\partial\theta}{\partial y}\right) - \frac{1}{\sigma}\tilde{\mu}\bar{T}_y\frac{\partial\theta}{\partial y}$$

$$-\left\{\frac{\bar{\rho}}{\bar{T}}L(\bar{T})+(\gamma-1)M^2\tilde{\mu}(\bar{u}_y)^2+\frac{1}{\sigma}(\tilde{\mu}\bar{T}_y)_y\right\}\theta=0, \tag{3.6}$$

$$\tilde{\rho}=-\frac{\bar{\rho}}{\bar{T}}\theta. \tag{3.7}$$

Here $\bar{\mu}=\bar{\mu}(\bar{T})$, $\tilde{\mu}=d\bar{\mu}/d\bar{T}$, and the operator $L(\ )$ is defined by

$$L(\ )=\bar{u}\frac{\partial}{\partial x}+\bar{v}\frac{\partial}{\partial y}.$$

In these equations, variables x and y have not yet been transformed into X and Y using (2.49). This will be done at a later stage.

So far we have not specified the size of the wavenumber a relative to the Mach number. We know from the analysis in §2 that the hypersonic boundary layer splits into two sublayers in the large Mach number limits: a wall layer of $O(M_1)$ thickness where $\bar{T}=O(M^2)$ and a temperature adjustment layer of $O(1)$ thickness sitting at the edge of the boundary layer where $\bar{T}=O(1)$. We note from (2.49) that

$$dy=\frac{b(X)}{\rho_1 T_1^{3/2}}\bar{T}d\eta.$$

Hence in terms of the physical variable y, the wall layer and the temperature adjustment layer are of thickness of $O(M^2M_1)$ and $O(1/M_1)$, respectively. Thus Görtler vortices trapped in the wall layer have large wavelength with $a=O(1/(M^2M_1))$; whilst Görtler vortices trapped in the temperature adjustment layer have shorter wavelength and have

$$a=O(\frac{1}{M_1}). \tag{3.8}$$

It can be shown that the growth rates for these two modes are respectively of order one and order $\sqrt{M^2M_1}$. Thus the mode trapped in the temperature adjustment layer is the most dangerous mode and will be studied in the rest of this paper.

4 The inviscid mode trapped in the temperature adjustment layer

As in the case when there is no pressure gradient (see Hall and Fu (1989)), an important term in the perturbation equations is that involving $L(\bar{v})$ in the y-momentum equation. It is easy to show with the aid of the basic state properties listed in the Appendix that

$$L(\bar{v})=-B(X)M^2+\cdots, \tag{4.1}$$

where the expression for $B(X)$ is given in the Appendix. This term requires the Görtler number to be of order M^2 (the wall curvature should first of all overcome the effective negative curvature of the basic state if Görtler vortices were to exist at all). Hence we scale G by writing

$$G = M^2\tilde{G}. \tag{4.2}$$

With the order of G fixed, we can now use the basic flow properties to deduce the relative orders of the perturbation quantities. It is found that

$$\frac{\partial}{\partial X} = O(\sqrt{M^2 M_1}), \quad V = O(W) = O(\sqrt{\frac{M^2}{M_1}}\theta), \quad P = O(\frac{M^2}{M_1}\theta), \tag{4.3}$$

and that U is of such an order that it does not enter the leading order analysis. The large growth rate implied by (4.3a) is driven by the term $L(\bar{v})' + \frac{1}{2}\kappa G\bar{u}^2$ in the y-momentum equation. This makes the viscous terms in the perturbation equations unimportant and so the resulting eigenvalue problem is essentially inviscid.

With the use of (4.1) and (4.2), we have

$$L(\bar{v}) + \frac{1}{2}\kappa G\bar{u}^2 = \left(\frac{1}{2}\kappa(x)\tilde{G} - B(x)\right) M^2.$$

Later we will show that if $\tilde{G}$ is chosen such that the coefficient of M^2 in the above equation vanishes and if the crossflow is zero, the $O(\sqrt{M^2 M_1})$ growth rate will become zero and $\frac{1}{2}\kappa(x)\tilde{G} = B(x)$ then defines the leading order neutral position (this is not true, however, when the crossflow is non-zero, as we shall show later). In the neighbourhood of this leading order neutral position, Görtler vortices have a smaller growth rate. Such near-neutral modes are dominated by viscous effects (see Hall and Fu (1989)).

We now turn to the determination of the order of crossflow amplitude. It can be seen from (3.2)−(3.7) that this is achieved by investigating the terms involving the operator

$$\bar{u}\frac{\partial}{\partial x} + \bar{v}\frac{\partial}{\partial y} + ia\bar{w}.$$

With the use of the asymptotic expressions listed in the Appendix, this operator can be written in the temperature adjustment layer as

$$U_1 B_1(1 - \cdots)\frac{\partial}{\partial X} + iaW_1(1 - \frac{M_1^{2\beta}}{M^2}\cdot\frac{c_2 T_1}{N}e^{\bar{y}} + \cdots). \tag{4.4}$$

to leading order. It may appear that crossflow effects will be felt when $\partial/\partial X \sim aW_1$, but it will be shown later that the leading order constant term in $\bar{w}$ does not affect the leading order growth rate, see Hall (1985) for a similar result for the incompressible problem. Therefore, the appropriate size of the crossflow is fixed by letting

$$\frac{\partial}{\partial X} \sim \frac{M_1^{2\beta}}{M^2}aW_1$$

and in view of (3.8) and (4.3a), this gives

$$W_1 \sim \frac{M^3}{M_1^{\frac{1}{2}+2\beta}}.$$

We thus introduce an $O(1)$ parameter δ by

$$W_1 = \frac{N}{c_2 T_1} \cdot \frac{M^3}{M_1^{\frac{1}{2}+2\beta}} \delta \tag{4.5}$$

to characterize the scaled crossflow amplitude. With the order of the crossflow fixed, we now look for the following form of WKB solutions for (3.2)-(3.7):

$$\begin{aligned} V &= \sqrt{\frac{M^2}{M_1}} \left(V_0(X,\tilde{y}) + \cdots\right) E + \cdots, \\ W &= \sqrt{\frac{M^2}{M_1}} \left(W_0(X,\tilde{y}) + \cdots\right) E + \cdots, \\ \theta &= \left(\theta_0(X,\tilde{y}) + \cdots\right) E + \cdots, \\ P &= \frac{M^2}{M_1} \left(P_0(X,\tilde{y}) + \cdots\right) E + \cdots, \end{aligned} \tag{4.6}$$

where E, defined by

$$E = \exp\left(\sqrt{M^2 M_1} \int^X \frac{\rho_1 \sqrt{T_1}}{b U_1 B_1} \lambda(X) dX - iaW_1 \int^X \frac{dX}{U_1 B_1}\right). \tag{4.7}$$

takes care of the fast variation of the perturbation quantities in the streamwise direction. Here $\lambda(X)$ is in general complex, the real part of it characterizes the growth rate of the disturbance. In each of the expansions in (4.6), the first ellipse represents the higher order terms which tends to zero as $M \to \infty$, whilst the second ellipse represents the meanflow correction and higher harmonics. We note that the larger constant term iaW_1 in (4.4) has been absorbed by inserting the second term in the expression for E. Thus, as remarked below (4.4), the term iaW_1 in $\bar{w}$ only contribute a sinusoidal coefficient to the disturbance without affecting the growth rate.

On substituting (4.6) into the linear perturbation equations (3.2)−(3.7) and make use of the basic state properties listed in the Appendix, we obtain, by keeping only those leading order terms,

$$-\frac{T_1}{\bar{T}} \frac{\partial V_0}{\partial \tilde{y}} + ikW_0 = 0, \tag{4.8}$$

$$(\lambda - ik\delta e^{\tilde{y}}) V_0 - \frac{\hat{G}}{\bar{T}} \theta_0 - \frac{1}{\rho_1} \frac{\partial P_0}{\partial \tilde{y}} = 0, \tag{4.9}$$

$$\frac{ik}{\rho_1}P_0 + \frac{T_1^2}{\bar{T}^2}\delta e^{\tilde{y}}V_0 + \frac{T_1}{\bar{T}}(\lambda - ik\delta e^{\tilde{y}})W_0 = 0, \tag{4.10}$$

$$-\frac{T_1^2}{\bar{T}}e^{\tilde{y}}V_0 + (\lambda - ik\delta e^{\tilde{y}})\theta_0 = 0. \tag{4.11}$$

where

$$k = \frac{b}{\rho_1\sqrt{T_1}}\frac{a}{M_1}, \quad \hat{G} = \frac{\rho_1\sqrt{T_1}}{b}\left(\frac{1}{2}\tilde{G}\kappa - B(X)\right). \tag{4.12}$$

It can be seen that the function $\hat{G}$ defined above represents a balance between the positive wall curvature and the negative curvature due to the basic state.

By eliminating W_0, θ_0 and P_0 from (4.8)–(4.11) in favour of V_0 and introducing a new independent variable ζ by

$$\zeta = e^{\tilde{y}}, \tag{4.13}$$

we obtain

$$\zeta^2\frac{\partial^2 V_0}{\partial\zeta^2} + \frac{\zeta(1-\zeta)}{1+\zeta}\frac{\partial V_0}{\partial\zeta} + H(\zeta)V_0 = 0, \tag{4.14}$$

where

$$H(\zeta) = \frac{ik\delta}{\lambda - ik\delta\zeta}\cdot\frac{\zeta(1-\zeta)}{1+\zeta} + k^2\left\{\frac{\hat{G}\zeta}{(\lambda - ik\delta\zeta)^2} - (1+\zeta)^2\right\}. \tag{4.15}$$

It is convenient to eliminate the first order derivative term from (4.14) by introducing $\hat{V}$ through

$$\hat{V} = \frac{\sqrt{\zeta}}{1+\zeta}V_0.$$

Equation (4.14) then reduces to

$$\zeta^2\frac{\partial^2 V}{\partial\zeta^2} + \left\{\frac{1}{4} + \frac{\zeta(1-\zeta)}{(1+\zeta)^2} + H(\zeta)\right\}V = 0, \tag{4.16}$$

where the 'hat' over V has been dropped to simplify notation. Under the transformation $\zeta = e^{\tilde{y}}$, $-\infty < \tilde{y} < \infty$ becomes $0 < \zeta < \infty$ and therefore equation (4.16) is to be solved subject to the asymptotic boundary conditions $V \to 0$ as $\zeta \to 0,\ \infty$. These conditions should be made more precise for numerical calculation and it can be deduced from (4.16) that the correct decay behaviour is

$$V \to \zeta^{\frac{1}{2}+k}\left\{1 - \frac{\zeta}{2k+1}[1 + \frac{ik\delta}{\lambda} + k^2(\frac{\hat{G}}{\lambda^2} - 2)] + O(\zeta^2)\right\} \quad \text{as } \zeta \to 0,$$

$$V \to \zeta^{-k}e^{-k\zeta}, \text{ as } \zeta \to \infty. \tag{4.17}$$

The eigenvalue problem (4.16) and (4.17) determines the relationship between λ (the real part of which is the growth rate), the scaled crossflow amplitude δ and the scaled wavenumber k. In addition, $\hat{G}$, defined by (4.12), can also be taken as a parameter for fixed X. We note

that for each set of fixed values of δ, k and $\hat{G}$, if (λ, V) is an eigenvalue set of (4.16) then so is $(-\lambda^*, V^*)$, where an asterisk denotes complex conjugate. Therefore to each unstable mode there corresponds a stable mode. Also, for each set of fixed values of k and $\hat{G}$, if (δ, λ, V) is an eigenvalue set of (4.16) then so is $(-\delta, -\lambda, V)$. Hence we can restrict our attention to positive crossflow parameters and will do so for the remainder of this paper.

Before we solve this eigenvalue problem for the non-zero crossflow cases, let us first note that when there is no crossflow, $\delta = 0$ and then (4.14) can be written as

$$\frac{\partial}{\partial\zeta}\left\{\frac{\zeta}{(1+\zeta)^2}\frac{\partial V_0}{\partial\zeta}\right\} + \frac{k^2}{\zeta(1+\zeta)^2}\left\{-(1+\zeta)^2 + \frac{\hat{G}}{\lambda^2}\zeta\right\}V_0 = 0. \tag{4.18}$$

Equation (4.18) subject to V_0 vanishing at $\zeta = 0,\ \infty$ is a standard Sturm-Liouville problem which can be taken to be an eigenvalue problem for $\hat{G}/\lambda^2$ for each fixed k. Its solution is of the form

$$\frac{\hat{G}}{\lambda^2} = F(k), \text{ i.e. } \lambda^2 = \frac{\hat{G}}{F(k)}, \tag{4.19}$$

where $F(k)$ is a positive function of the scaled wavenumber k and can easily be determined by solving (4.18) numerically using the fourth order Runge-Kutta method. This solution will be discussed further in the following section.

It follows from (4.19) that

$$\lambda^2 \geq 0 \text{ if } \hat{G} \geq 0, \qquad \lambda^2 \leq 0 \text{ if } \hat{G} \leq 0.$$

If we denote the location where $\hat{G} = 0$ by X_n, then λ is real on one side of X_n and is purely imaginary on the other side. This implies that as $X = X_n$ is crossed, the behaviour of the disturbance changes from being oscillatory to being exponentially growing. Thus we may define $X = X_n$ as the neutral position and in view of the definitions (4.2) and (4.12b), the corresponding neutral Görtler number G then expands as

$$G = \frac{2B(X_n)}{\kappa(X_n)}M^2 + \text{higher order terms}, \tag{4.20}$$

where the higher order terms can be obtained by following the procedure given in Hall and Fu (1989). However, our purpose in the present paper is not to determine the expression for the neutral Görtler number, but instead we wish to investigate how the existence of a crossflow would affect the growth rate of the inviscid mode described by the eigenvalue problem (4.16). To be more specific, one of our aims in this paper is to determine how the growth rate– wavenumber relation shown in (4.19) for zero crossflow is modified as the crossflow is gradually increased.

5 Numerical results for non-neutral modes

The eigenvalue problem (4.16) and (4.17) has been solved by using the fourth-order Runge-Kutta method to determine the dependence of the growth rate (the real part of λ) on the wavenumber k with δ fixed or on the crossflow amplitude δ with k fixed. The boundary $\zeta = 0$ is chosen to be some small number and $\zeta = \infty$ is replaced by a large number which is continuously adjusted for varying k and δ values (since as we will see later the eigenfunctions become more and more concentrated around the singular point as we approach neutral stability). At each end, V is chosen arbitrarily and $\partial V/\partial\zeta$ is then calculated from (4.17). We shoot from the two ends and match the solutions at an appropriate middle point where we impose the condition that $(1/V)\partial V/\partial\zeta$ has the same value from either side.

For increasingly small wavenumbers, the eigenfunctions become more and more spread into the whole boundary layer (as we would expect since as $k \to 0$ we are approaching the wall layer mode) and in particular the eigenfunctions vary rapidly near the wall. In this case, it is found convenient to introduce a scaled variable ξ through $\zeta = e^{\xi}$ for the calculations in the interval to the left of the matching point.

In order to be able to continue the calculations even when the mode becomes neutrally stable (i.e. when λ becomes purely imaginary), we also introduce an indentation in our integration path. In order to see whether the indented path should be above or below the real axis, we first note from (4.15) that the complex singular point of the governing equation is at ζ_c^* given by

$$\zeta_c^* = \frac{1}{k\lambda}(\lambda_i - \lambda_r i), \tag{5.1}$$

where $\lambda_r + i\lambda_i = \lambda$. For growing Görtler vortices $\lambda_r > 0$ and so this singular point lies below the real axis. Thus if the neutrally stable mode is taken to be approached from the unstable mode, then the integration path should be indented from above. In our calculations, the indentation is chosen to be a triangle and checks were duly made to make sure that it does not make any difference whether the indentation is on the left or right hand side of the matching point and how large the indentation is.

We now present our numerical results for the non-neutral modes. All of the following results correspond to $\hat{G} = 2$ and are for the first (i.e. the fundamental) mode. Other choices of positive $\hat{G}$ values can be shown to yield qualitatively similar results. The cases $\hat{G} \leq 0$ will be discussed in the final section. We note that although $\hat{G} \leq 0$ is a possibility, cases corresponding to $\hat{G} > 0$ are more important since when $\delta = 0$, positive values of $\hat{G}$ give rise to unstable Görtler vortices over the whole wavenumber regime, whilst if $\hat{G} \leq 0$, no unstable Görtler vortices can exist.

We shall first investigate the dependence of the growth rate on the wavenumber with

δ fixed. In Fig. 2(a) we have shown such growth rate curves for a number of δ values, including the zero-cross flow case $\delta = 0$. We see that for $\delta = 0$, the growth rate tends to zero as $k \to 0$ and tends to a constant as $k \to \infty$. The former behaviour is required as the present mode should match with the wall layer mode as $k \to 0$ and the wall layer mode has smaller growth rate. We now show that the latter behaviour is governed by a WKB solution of the governing equation (4.18).

When $\delta = 0$, Görtler vortices are governed by equation (4.18). As $k \to \infty$, we look for WKB solutions of the form

$$V_0 \sim \exp(k \int^{\zeta} E(\zeta) d\zeta).$$

Equation (4.18) requires that

$$\zeta^2 E^2(\zeta) = \frac{\hat{G}}{\lambda^2}\zeta - (1+\zeta)^2.$$

It then follows that in general there will be two first order turning points where $E(\zeta) = 0$. But the first mode which we are looking for must correspond to these two first order turning points coalescing to form a single second order turning point. This occurs when

$$(\frac{\hat{G}}{\lambda^2} - 2)^2 - 4 = 0,$$

which yields the only acceptable result

$$\lambda = \frac{\sqrt{\hat{G}}}{2}.$$

The corresponding second order turning point is then at $\zeta = 1$. In order to determine the higher order correction terms to the growth rate, we have to carry out the standard asymptotic analysis for second order turning point problems. Such an analysis shows that in the zero crossflow case λ expands as

$$\lambda = \frac{\sqrt{\hat{G}}}{2} - \frac{\sqrt{\hat{G}}}{16} \cdot k^{-1} + O(k^{-3/2}). \tag{5.2}$$

The dotted line shown in Fig. 2(a) corresponds to this asymptotic result. We note that the asymptotic analysis leading to (5.2) is very similar to that detailed in Fu, Hall and Blackaby (1992) for Sutherland's law fluids and that the growth rate curves for the two viscosity laws have the same structure but they are fundamentally different from the growth rate curve for incompressible Görtler vortices. We also note that the growth rate curve for $\delta = 0$ given in Fig. 2(a) is also consistent with those growth rate curves, obtained by Dando and Seddougui (1992), which emerged as the Mach number is gradually increased.

As δ is increased from zero gradually, we see from Fig. 2(a) that the growth rate is decreased at each fixed wavenumber and it no longer tends to a constant as $k \to \infty$ (this behaviour is also seen in Dando's (1992) $O(1)$ Mach number calculations). Instead, we see for $\delta = 0.1$ that there exists a critical wavenumber, k_{cr} say, at which the growth rate vanishes. Such critical wavenumbers also exist for other δ values (as can be seen from the exact solution to be discussed in the following section) although we are unable to show their existence in Fig. 2(a) due to numerical difficulty. For $k > k_{cr}$, no solution can be found (since if a stable mode could be found, then an unstable mode could also exist). Thus at each δ value, Görtler vortices are unstable in the wavenumber regime $(0, k_{cr})$, stable in the wavenumber regime (k_{cr}, ∞) and are neutrally stable at $k = k_{cr}$.

Fig. 2(b) shows seven more neutral curves for the larger δ values indicated. We see that whilst for small δ values crossflow effects are stabilizing over the whole wavenumber regime, this is no longer the case for large enough δ values. Fig. 2(b) shows that crossflow effects are actually destabilizing over the small wavenumber regime whilst remaining stabilizing over the large wavenumber regime. We note that as $\delta \to \infty$, the critical wavenumber k_{cr} at which $\lambda_r = 0$ tends to a definite limit. We shall show in the next section that this limiting value is given by 1/4. Hence we can deduce that for large δ values, unstable Görtler vortices can only exist in the wavenumber regime $(0, \frac{1}{4})$ and that for any Görtler vortex with a wavenumber lying in the region $(\frac{1}{4}, \infty)$, there always exists a δ value at which the vortex is completely stabilized.

For Görtler vortices with wavenumber lying in the region $(0, \frac{1}{4})$, numerical calculations show that $\lambda = O(\delta)$, as $\delta \to \infty$. Therefore in the large crossflow limit, we can look for the following asymptotic solutions for (4.16) and (4.17):

$$\lambda = \lambda_0 \delta + \lambda_1 + \lambda_2 \delta^{-1} + \cdots,$$

$$V(X, \zeta) = V_0(X, \zeta) + \delta^{-1} V_1(X, \zeta) + \cdots. \tag{5.3}$$

By substituting (5.3) into (4.16) and (4.17), it is easy to show that λ_0 and V_0 are determined by the eigenvalue problem

$$\zeta^2 \frac{\partial^2 V_0}{\partial \zeta^2} + \left\{ \frac{1}{4} + \frac{\zeta(1-\zeta)}{(1+\zeta)^2} + \frac{ik}{\lambda_0 - ik\zeta} \cdot \frac{\zeta(1-\zeta)}{1+\zeta} - k^2(1+\zeta)^2 \right\} V_0 = 0,$$

$$V_0 \to \zeta^{\frac{1}{2}+k} \left\{ 1 - \frac{\zeta}{1+2k}[1 + \frac{ik}{\lambda_0} - 2k^2] + O(\zeta^2) \right\}, \quad \text{as } \zeta \to 0, \tag{5.4}$$

$$V_0 \to \zeta^{-k} \mathrm{e}^{-k\zeta}, \quad \text{as } \zeta \to \infty.$$

We see that this reduced eigenvalue problem is now independent of $\hat{G}$ and hence the Görtler vortices in the wavenumber regime $(0, \frac{1}{4})$ can appropriately be identified as crossflow vortices

since in the large crossflow limit, their existence is dictated by the crossflow instead of by the wall curvature effects. The eigenvalue problem (5.4) can be solved numerically to determine the dependence of λ_0 on the wavenumber k, but we shall not present the corresponding results here since these results merely confirm the large crossflow behaviour of those growth rate curves shown in Fig. 2(b).

In Figures 3(a, b), we have shown the dependence of the imaginary part of λ on the wavenumber for the same δ values as those used in Figures 2(a, b). We can see that $\lambda_i > 0$ for $\lambda_r \geq 0$, which implies that when $\lambda_r = 0$, the critical point defined by (5.1) lies in the interval of integration and thus the neutral mode (to be studied in the following section) has a critical layer structure.

In order to see the dependence of the growth rate on the crossflow for fixed wavenumbers, we have shown in Figures 4(a,b) the growth rate curves in the (λ_r, δ) plane for a selection of k values. We can immediately draw the following conclusions. For each fixed k value greater than $1/4$, there exists an unique critical δ value, δ_{cr} say, such that $\lambda_r > 0$ for $0 < \delta < \delta_{cr}$, $\lambda_r = 0$ at $\delta = \delta_{cr}$, and there is no solution for $\delta > \delta_{cr}$. For $k < 1/4$, we always have $\lambda_r > 0$, which confirms the findings shown in Fig. 2(b) that Görtler vortices with wavenumber lying in $(0, \frac{1}{4})$ are always unstable. For $k = 1/4$, neutral stability is attained at $\delta_{cr} = \infty$. Figures 5(a,b) show the dependence of the imaginary part of λ on the crossflow for the same k values used in Figures 4(a,b). Here again we have $\lambda_i > 0$. In Figures 6(a,b), we have shown the evolution of the real and imaginary parts of V for fixed values $\delta = 0.2, \hat{G} = 2$ as k is increased. We can see that a critical layer structure is gradually emerging as k is increased towards the neutral value k_{cr}.

6 The neutrally stable mode

Numerical results presented in the previous section suggest that to each δ value, there corresponds a critical k value at which neutral stability occurs and for each k value greater than $1/4$, there again exists a critical δ value at which neutral stability is achieved. In this section, we shall determine the relation between k and δ when neutral stability occurs.

When Görtler vortices are neutrally stable, we have $\lambda_r = 0$ and so we may write

$$\lambda = i\hat{\lambda}, \tag{6.1}$$

where $\hat{\lambda}$ is real and from our previous numerical results we know it is also positive. In the present neutral case, the governing equation (4.16) may be written as

$$\zeta^2 \frac{\partial^2 V}{\partial \zeta^2} + \left\{ \frac{1}{4} + \frac{\zeta(1-\zeta)}{(1+\zeta)^2} - \frac{1}{\zeta - \zeta_c} \cdot \frac{\zeta(1-\zeta)}{1+\zeta} - \frac{\hat{G}\zeta}{\delta^2(\zeta - \zeta_c)^2} - k^2(1+\zeta)^2 \right\} V = 0, \tag{6.2}$$

where

$$\zeta_c = \frac{\hat{\lambda}}{k\delta} > 0. \tag{6.3}$$

This equation has a regular singular point at $\zeta = \zeta_c$ and in the neighbourhood of this singular point the two Frobenius solutions can easily be shown to be given by

$$V = V_\pm = (\zeta - \zeta_c)^{\frac{1}{2}(1\pm\nu)} \left\{ 1 + \frac{1}{(1\pm\nu)\zeta_c} \left(\frac{1-\zeta_c}{1+\zeta_c} - \frac{\hat{G}}{\zeta_c \delta^2} \right) (\zeta - \zeta_c) + \cdots \right\}, \tag{6.4}$$

where

$$\nu = \sqrt{1 + \frac{4\hat{G}}{\zeta_c \delta^2}} = \sqrt{1 + \frac{4k\hat{G}}{\delta\hat{\lambda}}}. \tag{6.5}$$

In general, the solution in the neighbourhood of the singular point would be given by $AV_+ + BV_-$, a linear combination of V_+ and V_-, but for the present neutral problem, we can show that either A or B must be zero.

To the above end, we use Mile's (1961) approach and consider a function $\tau(X, \zeta)$ defined by

$$\tau(X, \zeta) = (V'V^*)_i, \tag{6.6}$$

where a subscript i signifies taking the imaginary part and a prime denotes partial differentiation with respect to ζ. It is straightforward to show with the aid of (6.2) that $\partial\tau/\partial\zeta = 0$. Thus τ can only be a function of X only. But we know $\tau(X, 0) = \tau(\infty) = 0$ and so $\tau(X, \zeta) \equiv 0$.

However, if

$$V = AV_+ + BV_-, \tag{6.7}$$

we then have

$$\tau = (AB^* V_+' V_-^* + A^* B V_-' V_+^*)_i. \tag{6.8}$$

As we have argued in the previous section, if the neutral mode is taken to be the limit of the unstable modes, then the branch cut should be in the + plane. We therefore have

$$\mathrm{Arg}(\zeta - \zeta_c) = \begin{cases} 0 & \zeta - \zeta_c > 0, \\ \pi, & \zeta - \zeta_c < 0, \end{cases}$$

and

$$(\zeta - \zeta_c)^{\frac{1}{2}(1\pm\nu)} = |\zeta - \zeta_c|^{\frac{1}{2}(1\pm\nu)} \mathrm{e}^{i\frac{\pi}{2}(1\pm\nu)S}, \tag{6.9}$$

where

$$S = \begin{cases} 0, & \zeta - \zeta_c > 0, \\ 1, & \zeta - \zeta_c < 0. \end{cases} \tag{6.10}$$

Hence we have

$$V_\pm^* = V_\pm \mathrm{e}^{-i\pi(1\pm\nu)S}. \tag{6.11}$$

On substituting (6.11) into (6.8), and making use of the result $V_+'V_- - V_+V_-' = \nu$, we obtain

$$\tau = \left\{AB^*\nu e^{i\pi(1+\nu)S}\right\}_i.$$

Hence by evaluating the above expression on the left and right hand sides of ζ_c, we obtain

$$(AB^*)_i = 0 \quad \text{and} \quad (AB^*e^{i\pi(1+\nu)})_i = 0,$$

which imply that $AB^* = 0$ whenever $\sin\pi\nu \neq 0$ and so either A or B must vanish if ν is not an integer (our numerical results show this is also true even when ν is not an integer).

Once we have established this result, we can determine whether the solution is AV_+ or BV_- with the aid of the numerical solutions for the neutral mode (as the limit of our non-neutral calculations discussed in the previous section). The numerical results for $\hat{G} > 0$ show that the eigenfunctions are singular at the critical point and thus we deduce from (6.4) that the solution is always given by BV_- (since $\nu > 1$ when $\hat{G} > 0$ and V_+ is regular). This can also be verified by calculating the phase jumps across the critical point of the eigenfunctions; we then find that the phase jump is always $\pi(1-\nu)/2$ instead of $\pi(1+\nu)/2$. Here ν is calculated from (6.5). In the course of calculating these phase jumps for a selection of k values, we noticed the possibility $\nu = 4k$ and this was then verified by calculations for a wide range of wavenumbers. This result then points to the possible existence of an exact solution to the neutral eigenvalue problem (6.2). After some manipulation, such an analytical solution is found to indeed exist and is given by

$$\begin{aligned} &\nu = 4k, \quad \zeta_c = \frac{1}{4k}, \quad \delta = 4\hat{\lambda} \\ &16\hat{G}k = (16k^2 - 1)\delta^2, \qquad (6.12) \\ &V = B\zeta^{\frac{1}{2}}(\zeta - \zeta_c)^{\frac{1}{2}-2k}(\zeta + 1)^{-1}e^{-k\zeta}. \end{aligned}$$

We note that each component in the product on the right hand side of (6.12c) has a distinct role: they in turn represent the behaviour of the eigenfunction at the four regular singular points $\zeta = 0$, ζ_c, -1, and ∞.

The exact solution (6.12) can explain quite a few points about our numerical results. Firstly, we can see from (6.12d) that $k = 1/4$ is an important value. For any fixed $\hat{G} > 0$, neutral states can only be obtained for $k > 1/4$ since (6.12d) does not have a solution for δ otherwise. When $k = 1/4$, the neutral state is obtained at $\delta = \infty$. Secondly, for a given δ value, there exists a neutral k value (i.e. a k_{cr} at which $\lambda_r = 0$) and for a given k value greater than $1/4$, there exists a neutral δ value. All these conclusions certainly agree with the numerical results presented in Figures 2-5. Finally, we see from (6.12b) that even for moderate values of k, ζ_c can be quite small and in these cases the eigenfunctions become

trapped near the wall, which give rise to some numerical difficulties. This is why we have not extended the growth rate curves to the neutral points in Fig. 2(a) although we have done so in Fig. 2(b).

After having succeeded in obtaining the above exact neutral mode solution, we also considered the neutral mode eigenvalue problem formulated, but unsolved, by Bassom and Hall (1991). As remarked by these authors, their equation (2.14b) is just a scaled version of their equation (4.10c) and it governs the large wavenumber inviscid neutral mode. It suffices to consider their equation (4.10c), which can be written as

$$\frac{d^2\bar{V}_0}{d\psi^2} - \left\{1 + \frac{2}{\psi(\psi-\psi_c)} + \frac{1}{\hat{\lambda}^2\psi(\psi-\psi_c)^2}\right\}\bar{V}_0 = 0, \tag{6.13}$$

where $\psi_c = -\hat{\beta}/\hat{\lambda}$. Using the same procedure as that used in obtaining (6.12), we found that (6.13) also has an exact solution, given by

$$\hat{\lambda} = -\hat{\beta} = \frac{1}{\sqrt{2}}, \quad \bar{V}_0 = A\psi(\psi-\psi_c)^{-1}\mathrm{e}^{-\psi}, \tag{6.14}$$

where A is an arbitrary constant.

The eigenvalue problem associated with (6.13) arises in Bassom and Hall (1991) where the re-emergence of the Görtler vortex mode is considered at high scaled crossflow and vortex wavenumbers. In that paper it was found that at sufficiently high crossflow values the Görtler mode is stabilized over a finite band of nonzero wavenumbers. This stable band of wavenumbers increases with the crossflow; its left-hand limit approaches that of the stationary crossflow vortex of Gregory, Stuart and Walker (1955), while its right-hand limit is described by the inviscid eigenvalue problem associated with (2.14b) of Bassom and Hall (1991). The result (6.13) shows that, in the notation of Bassom and Hall (1991), the upper neutral wavenumber is related to the crossflow parameter λ by

$$\lambda = 2\sqrt{2}a^{1/2}\left(\frac{\bar{u}'(0)^2}{\bar{w}'(0)}\right)R^{-1/2}G^{1/2}. \tag{6.15}$$

Here R and G are the Reynolds and Görtler numbers whereas the unperturbed boundary layer is $(\bar{u}, R^{-1/2}\bar{v}, \lambda\bar{w})$. The prediction (6.15) is in excellent agreement with the numerical results of Bassom and Hall (1991) thus for example the result (6.15) differs from the computed value of a by less than 5% when $\lambda R^{1/2}G^{-1/2} = 4.75$.

7 Conclusion

So far, we have consistently assumed that $\hat{G} > 0$. We have shown that if $\delta = 0$, unstable Görtler vortices can exist in the whole wavenumber regime. But as δ is increased gradually from zero, this $(0, \infty)$ unstable wavenumber regime contracts to $(0, k)$ where k is related to δ by (6.12d) and tends to $1/4$ as δ tends to infinity. Any Görtler vortex with a wavenumber greater than $1/4$ could be completely stabilized by a large enough crossflow in the basic state. We have also shown that Görtler vortices over the wavenumber regime $(0, \frac{1}{4})$ are always unstable and for large crossflows they are actually destabilized by the crossflow. Since such Görtler vortices for large crossflows are no longer controlled by wall curvature effects, we have identified them more appropriately as crossflow vortices.

To complete our discussions, we now investigate what happens if $\hat{G} \leq 0$. In the zero-crossflow case, result (4.19) shows that if $\hat{G} \leq 0$, the inviscid mode has $\lambda_r = 0$ and so the growth rate curve in the (k, λ_r) plane is simply the k-axis. We now investigate how this curve (i.e. the k-axis) evolves as we increases δ gradually. We note that the neutral solution (6.12) is also valid for $\hat{G} \leq 0$. When $\hat{G} < 0$, we deduce from (6.12d) that for each δ value, there exists an unique k, k_{cr} say, at which $\lambda_r = 0$, and we must have $k_{cr} < 1/4$. This is verified by the numerical results shown in Figure 7(a,b) where we have shown two typical growth rate curves corresponding to $\delta = 5, 7$ and to $\hat{G} = -2$. It can be seen that for $\delta > 0$ and $\hat{G} < 0$, the only unstable wavenumber regime is now $(0, k_{cr})$ with $k_{cr} < 1/4$, which is even narrower than that for $\hat{G} > 0$. This is a result of the crossflow trying to destabilize and the negative *resultant* curvature trying to stabilize these (crossflow) vortices. It can be deduced from (6.12d), and it is also confirmed by Fig. 7, that k_{cr} tends to $1/4$ from below as $\delta \to \infty$, in contrast to the situation for $\hat{G} > 0$ where k_{cr} tends to $1/4$ from above as $\delta \to \infty$.

Figures 8(a,b) show that a crossflow vortex at a fixed δ value and with wavenumber lying in the region $(0, \frac{1}{4})$ can be completely stabilized by decreasing $\hat{G}$, and so although the crossflow vortices in the wavenumber regime $(0, \frac{1}{4})$ are always unstable for $\hat{G} > 0$, they can be nevertheless completely destroyed by a large enough resultant *negative* curvature (represented by $\hat{G}$). Therefore, crossflows stabilize the unstable Görtler vortices with wavenumber lying in the region $(1/4, \infty)$ and the negative resultant curvature stabilizes the unstable crossflow vortices with wavenumber lying the region $(0, 1/4)$.

To summarize, we have shown in this paper that in the hypersonic context, the crossflow which can completely stabilize the inviscid Görtler vortices considered must necessarily be of order

$$R^{-1/2} \frac{M^3}{M^{\frac{1}{2}+2\beta}}$$

in terms of the original physical variable. Within this order, we have shown at precisely what

crossflow value a Görtler vortex with a given wavenumber will be completely stabilized. It is seen that large wavenumber Görtler vortices can be stabilized more easily than smaller wavenumber Görtler vortices. This may imply that in practical situations small wavenumber Görtler vortices could be excited more easily than Görtler vortices with larger wavenumbers.

It is also seen that crossflow effects on Görtler vortices are fundamentally different for incompressible and hypersonic flows. For incompressible flows, Bassom and Hall (1991) showed that only at sufficiently large crossflow values, were Görtler vortices stabilized over a finite band of wavenumbers, whilst we have shown in this paper that for any non-zero crossflow, hypersonic Görtler vortices are stabilized over a semi-infinite wavenumber regime (k_{cr}, ∞), where k_{cr} is determined by the exact solution (6.12d) (with k_{cr} identified with the k there).

We have also shown that in order to quantify vortices' response to crossflow effects, the scaled wavenumber regime may be neatly divided into two regions: $(0, 1/4)$ and $(1/4, \infty)$. We have identified the vortices wavenumber lying in the first region as crossflow vortices since in the large crossflow limit, their existence is no longer supported by curvature effects but instead by the crossflow. We have also found the exact solution to the neutrally stable mode. This exact solution should be useful for studying the nonlinear development of Görtler vortices which is now under consideration.

REFERENCES

1. Bassom, A.P. and Hall, P. (1991), *Vortex instability in three-dimensional boundary layers: the relation between Görtler and crossflow vortices.* J. Fluid Mech. **232**, 647-680

2. Dando A. (1992), *The inviscid compressible Görtler problem in three-dimensional boundary layers.* Theoret. Comput. Fluid Dynamics. **3**, 253-265.

3. Dando, A. and Seddougui, S.O. (1992) *The inviscid compressible Görtler problem.* To appear in IMA J. Appl. Math. **3**, 253-265.

4 Fu, Y.B., Hall, P. and Blackaby, N.D. (1992), *On the Görtler instability in hypersonic flows: Sutherland's law fluids and real gas effects.* To appear in Phil. Trans. Royal Soc. Lond.

5 Fu, Y.B. and Hall, P. (1992a). *Nonlinear development and secondary instability of large-amplitude Görtler vortices in hypersonic boundary layers.* To apper in Euro. J. of Fluid Mech.

6 Fu, Y.B. and Hall, P. (1992b). *Effects of Görtler Vortices, Wall Cooling and Gas Dissociation on the Rayleigh Instability in a Hypersonic Boundary Layer.* To appear in J. Fluid Mech.

7 Gregory, N., Stuart, J.T. and Walker, W.S. (1955). *On the stability of three dimensional boundary layers with application to the flow due to a rotating disk.* Phil. Trans. R. Soc. Lond. **A248**, 155-494.

8. Hall, P. (1985). *The Görtler vortex instability mechanism in three-dimensional boundary layers.* Proc. R. Soc. Lond. **A399**, 135-152.

9. Hall, P. and Fu, Y.B. (1989). *On the Görtler vortex instability mechanism at hypersonic speeds.* Theoret. Comput. Fluid Dynamics, **1**,125-134.

10 Hall, P. (1990). *Görtler vortices in growing boundary layers: The leading edge receptivity problem, linear growth and the nonlinear breakdown stage*, Mathematika, **37**, 151-189.

11. Hall, P. and Malik M.R. (1987). *Görtler vortices in compressible boundary layers.* J. Eng.. Math. **23**, 239

12. Miles, J.W. (1961). *On the stability of heterogeneous shear flows.* J. Fluid mech. **10**, 496-508.

13. Stewartson, K. (1964). *The Theory of Laminar Boundary Layers in Compressible Flows.* Clarendon Press, Oxford.

Appendix: Basic state properties in the temperature adjustment layer

$$\bar{u} = U_1 f'(\eta) = U_1 \left\{ 1 + \left(\frac{1}{2}(n-1)c_2 M^{2\beta} - c_1 \right) \frac{T_1 e^{\tilde{y}}}{N M^2} + \cdots \right\}, \tag{A1}$$

$$\bar{w} = W_1 g(\eta) = W_1 \left(1 - \frac{c^2 T_1 e^{\tilde{y}}}{N} \frac{M_1^{2\beta}}{M^2} + \cdots \right), \tag{A2}$$

$$\bar{u}\frac{\partial}{\partial x} + \bar{v}\frac{\partial}{\partial y} = L(\ ) = U_1 B_1 f'(\eta)\frac{\partial}{\partial X} - U_1 B_1 f(\eta)\frac{a'(X)}{a(X)}\frac{\partial}{\partial \eta}, \tag{A3}$$

$$L(\bar{u}) = \max\left\{ O\left((n-1)\frac{M^{2+2\beta}}{M^2} \right),\ O\left(\frac{M_1^2}{M^2} \right) \right\}, \quad L(\bar{v}) = -B(X)M^2 + \cdots, \tag{A4}$$

$$\frac{\partial}{\partial x} = -\frac{B_4}{\bar{T}} M_1 M^2 \frac{\partial}{\partial \tilde{y}} + \cdots, \quad \frac{\partial}{\partial y} = -\frac{\rho_1 T_1^{3/2}}{b\bar{T}} M_1 \frac{\partial}{\partial \tilde{y}} + \cdots, \tag{A5}$$

$$\bar{u}_x = \max\left\{ O((n-1)M_1^{1+2\beta}),\ O(M_1) \right\}, \tag{A6}$$

$$\bar{u}_y = \max\left\{ O\left((n-1)\frac{M^{1+2\beta}}{M^2} \right),\ O\left(\frac{M_1}{M^2} \right) \right\}, \tag{A7}$$

$$\bar{v}_x = O(M^2 M_1^2), \quad \bar{v}_y = O(\bar{u}_x), \quad \bar{u}_x + \bar{v}_y = O(M_1^2), \tag{A8}$$

$$\bar{w}_x = O(W_1 M_1^{1+2\beta}), \quad \bar{u}_y = O\left(W_1 \frac{M_1^{2+2\beta}}{M^2} \right), \tag{A9}$$

$$\bar{T}_x = -\frac{B_4 T_1 e^{\tilde{y}}}{\bar{T}} M_1 M^2 + \cdots, \quad \bar{T}_y = -\frac{\rho_1 T_1^{5/2} e^{\tilde{y}}}{b\bar{T}} M_1 + \cdots, \tag{A10}$$

where

$$B_1 = \rho_1 T_1^{3/2}, \quad B_2 = \frac{b}{\sqrt{T_1}} \frac{d}{dx}\left(\frac{\sqrt{T_1}}{b} \right),$$

$$B_3 = -\frac{1}{2\beta}(\gamma - 1)\cos^2 \wedge \int_0^\infty (f''' + f f'') d\eta.$$

$$B_4 = B_3\left(\frac{P_1'}{P_1} + B_2 \right), \quad B(X) = U_1 B_1 \frac{\partial}{\partial X}\left\{ \frac{b B_4}{B_1} \right\}.$$

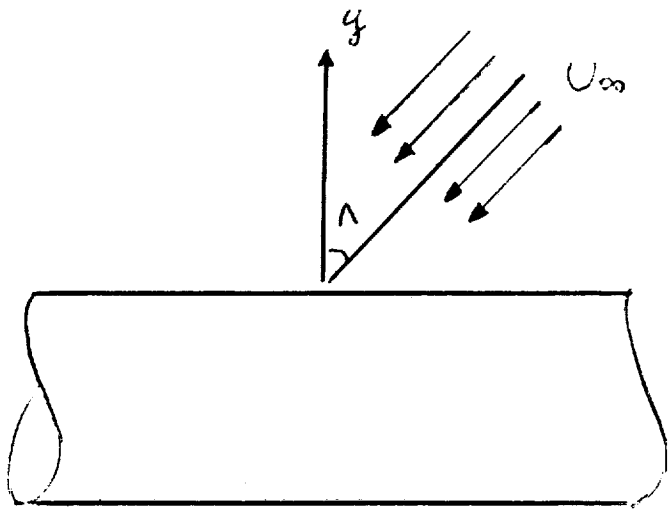

Figure 1. A typical example of a three-dimensional boundary layer: a boundary layer over a swept aerofoil.

Fig. 2(a)

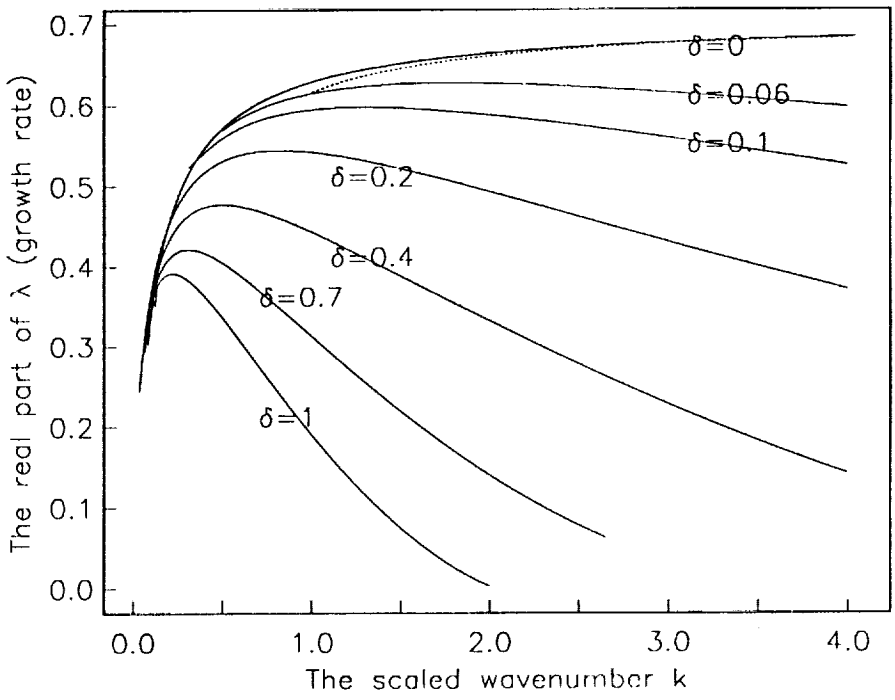

Fig. 2(b)

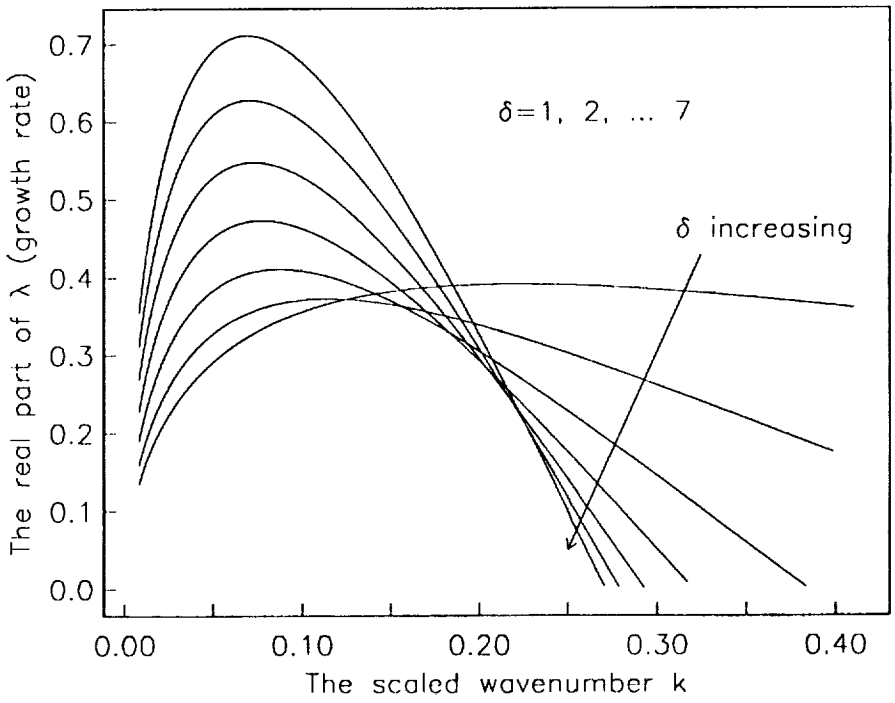

Figure 2. Dependence of the growth rate on the scaled wavenumber for $\hat{G} = 2$. (a) For small crossflows $\delta = 0, 0.06, 0.1, 0.2, 0.7, 1.$; the dotted line is the asymptotic result for $\delta = 0$ given by (5.2); (b) For larger crossflows $\delta = 1, 2, 3, ..., 7$.

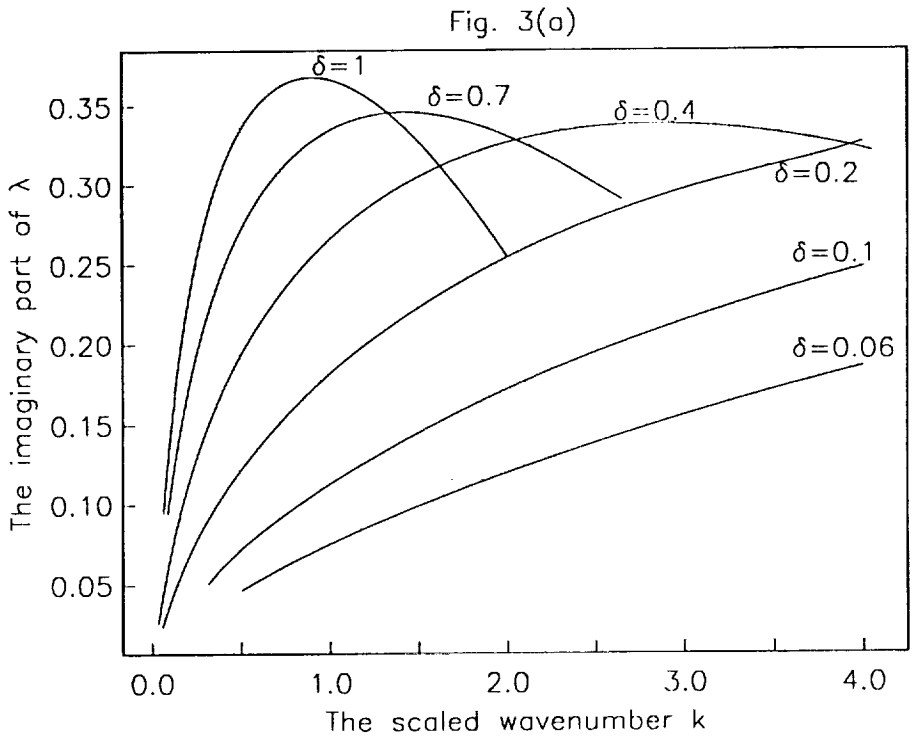

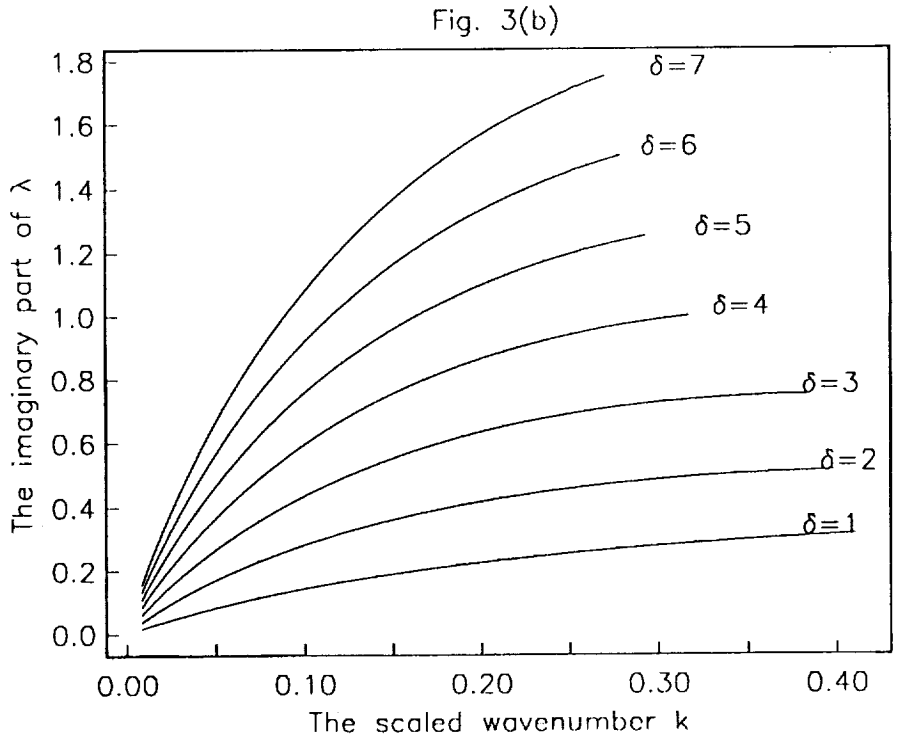

Figure 3. Dependence of the imaginary part of λ on the scaled wavenumber for $\hat{G} = 2$. (a) For small crossflows $\delta = 0, 0.06, 0.1, 0.2, 0.7, 1.$; (b) For larger crossflows $\delta = 1, 2, 3, ..., 7$.

Fig. 4(a)

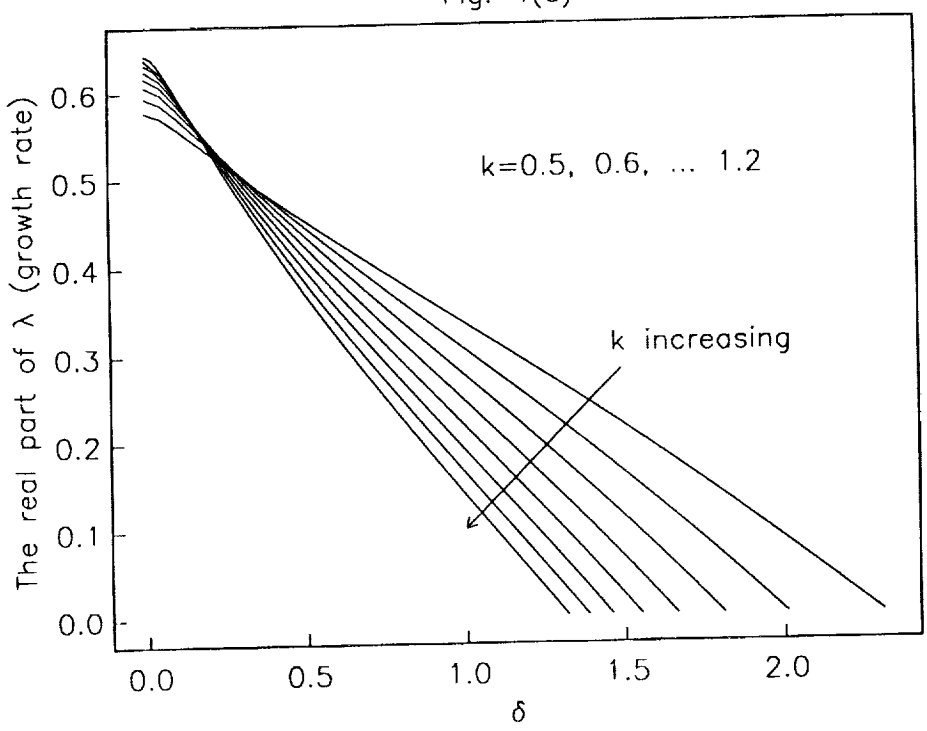

Fig. 4(b)

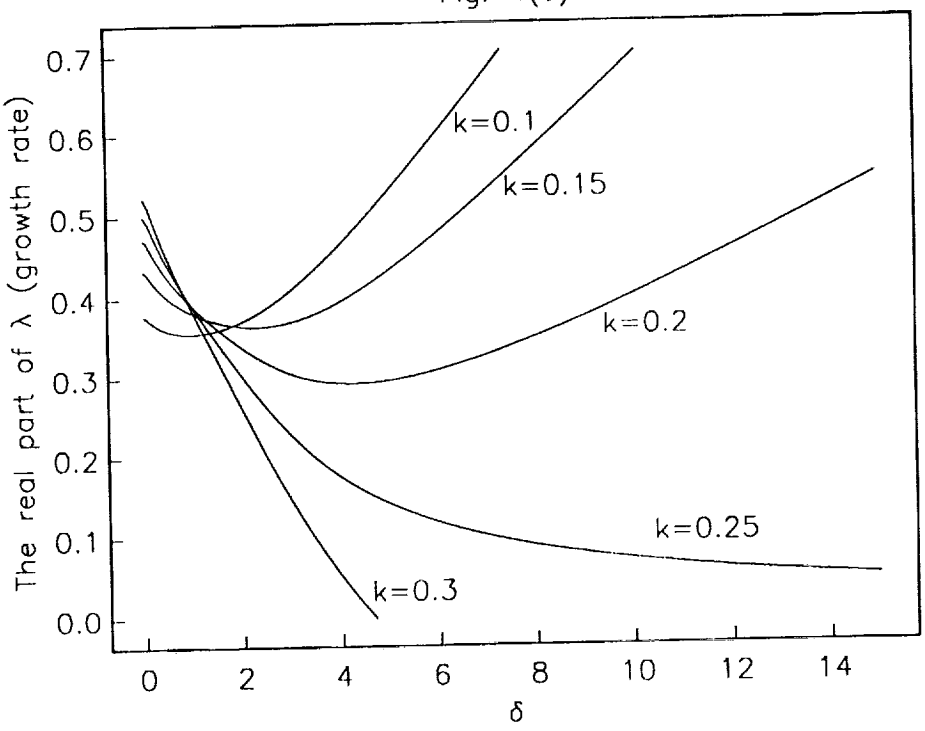

Figure 4. Dependence of the growth rate on the crossflow amplitude for $\hat{G} = 2$. (a) For $k = 0.5, 0.6, 0.7, ..., 1.2$ (all larger that 1/4); (b) for k=0.1, 0.15, 0.2, 0.25, 0.3.

Fig. 5(a)

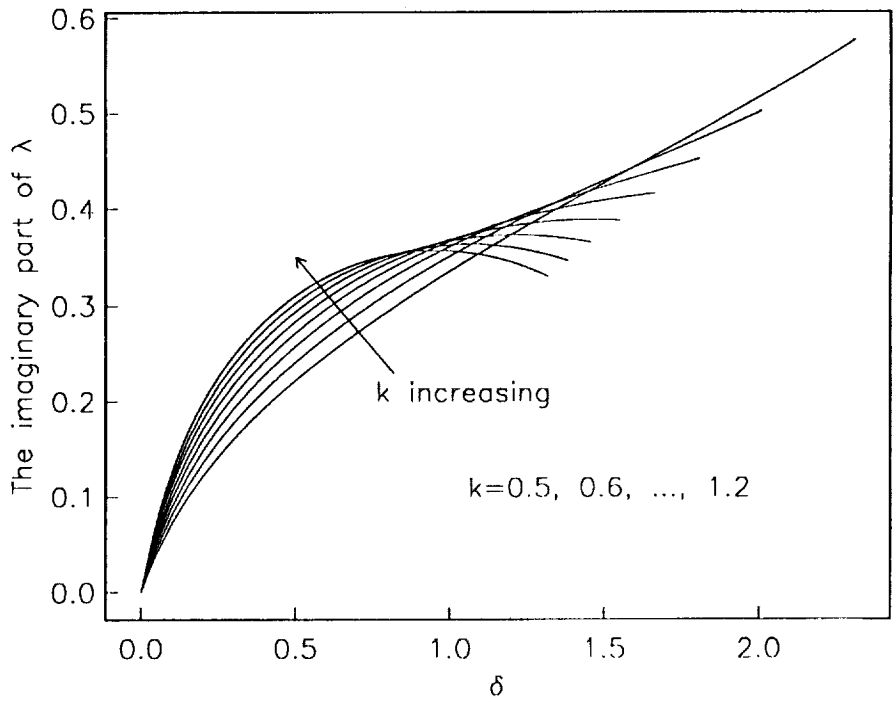

Fig. 5(b)

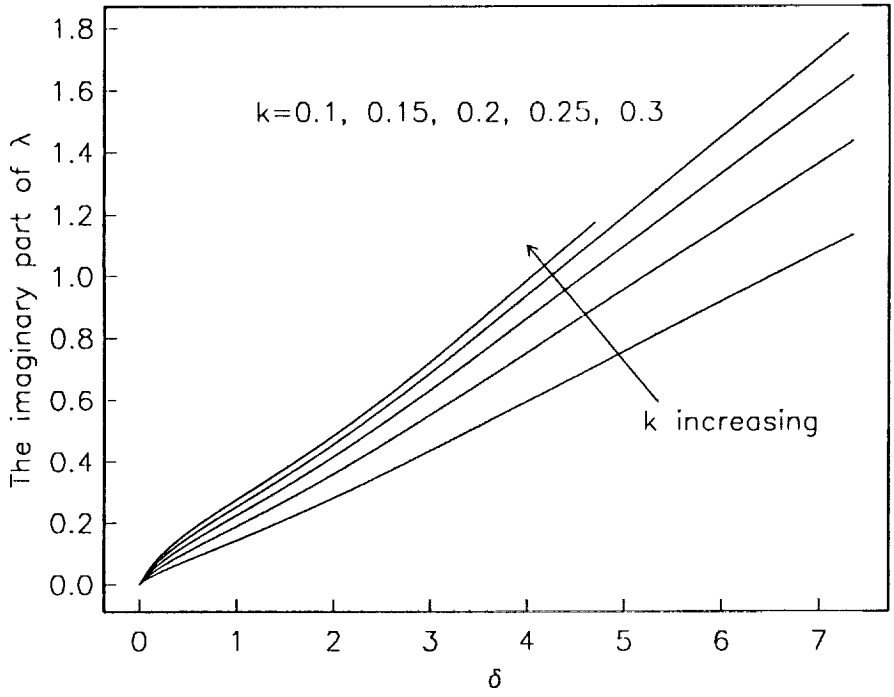

Figure 5. Dependence of the imaginary part of λ on the crossflow amplitude for $\hat{G} = 2$. (a) For $k = 0.5, 0.6, 0.7, ..., 1.2$; (b)for k=0.1, 0.15, 0.2, 0.25, 0.3.

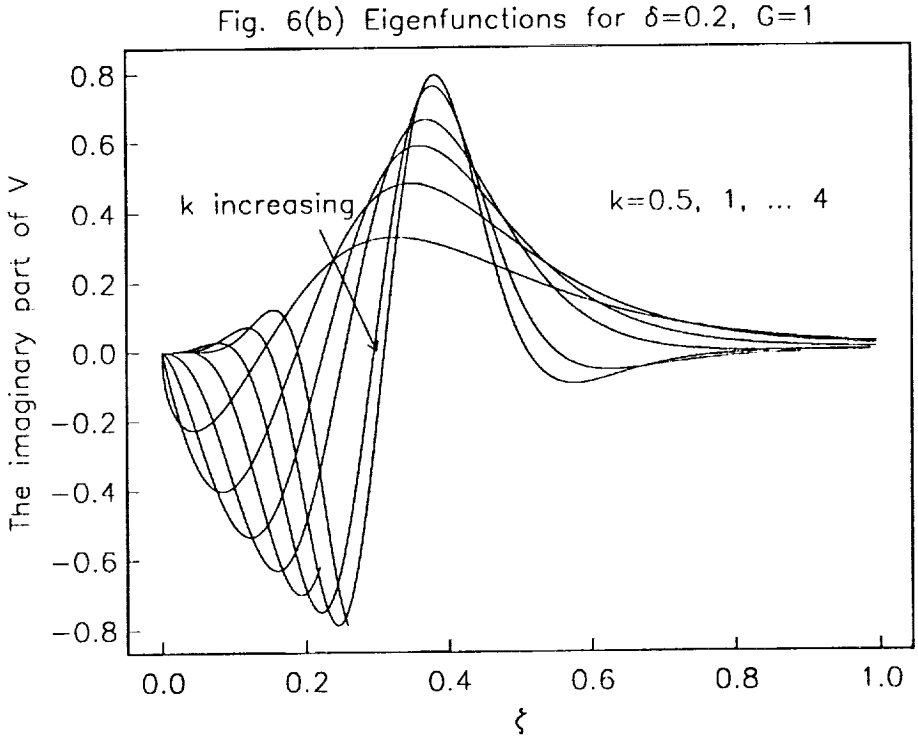

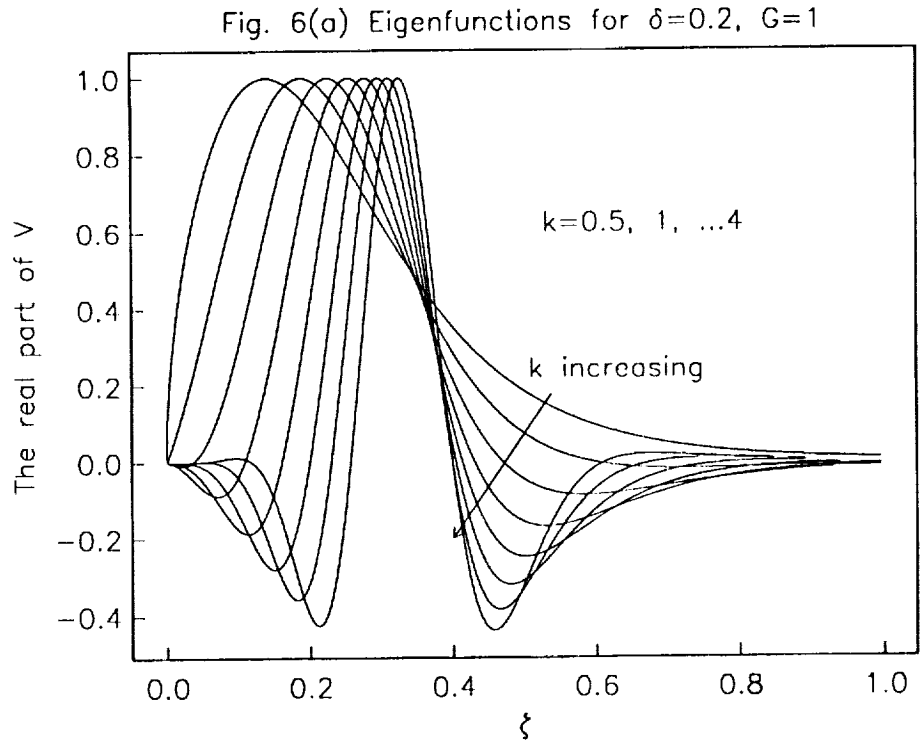

Figure 6. Variation of the eigenfunction for $\hat{G} = 2$ and $\delta = 0.2$ as k is increased towards the neutral value, showing the emergence of a critical layer structure. (a) The real part of V; (b) the imaginary part of V.

Fig. 7(a)

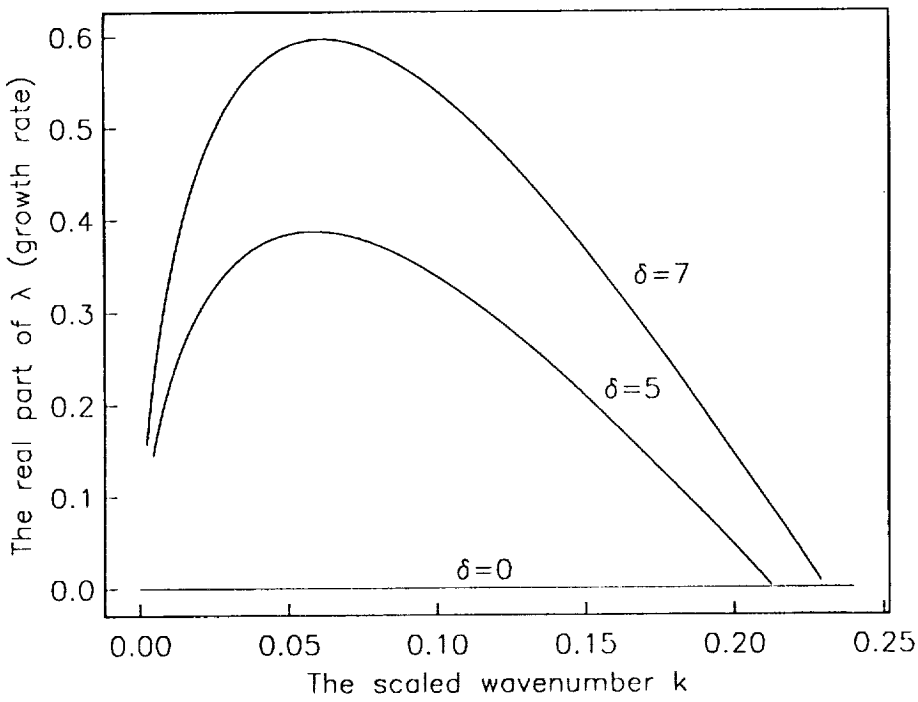

Fig. 7(b)

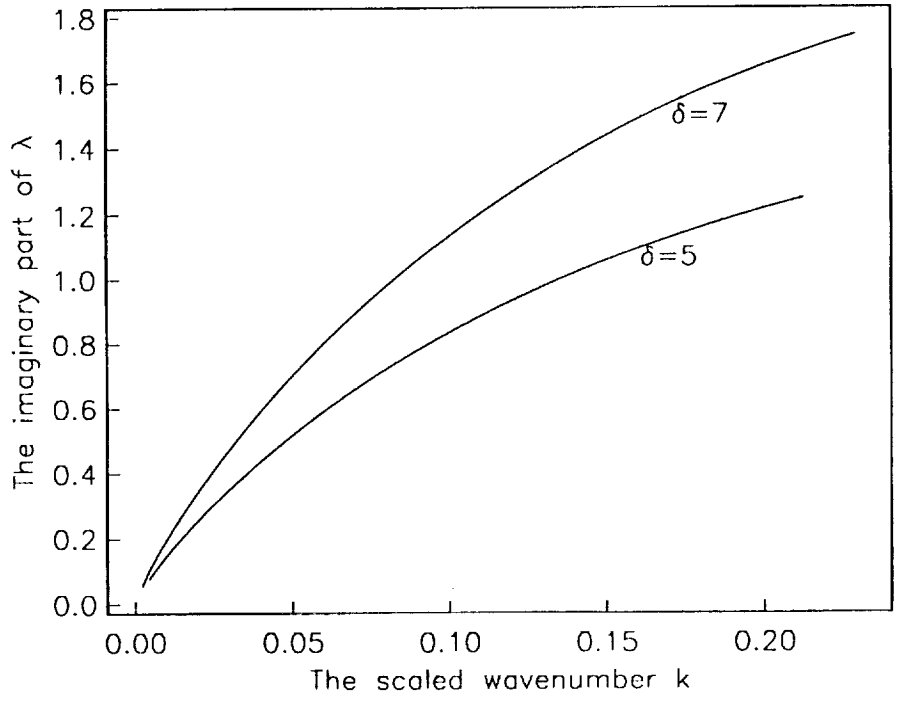

Figure 7. Dependence of (a) the growth rate and (b) the imaginary part of λ on the scaled wavenumber for $\hat{G} = -2$ and $\delta = 5, 7$.

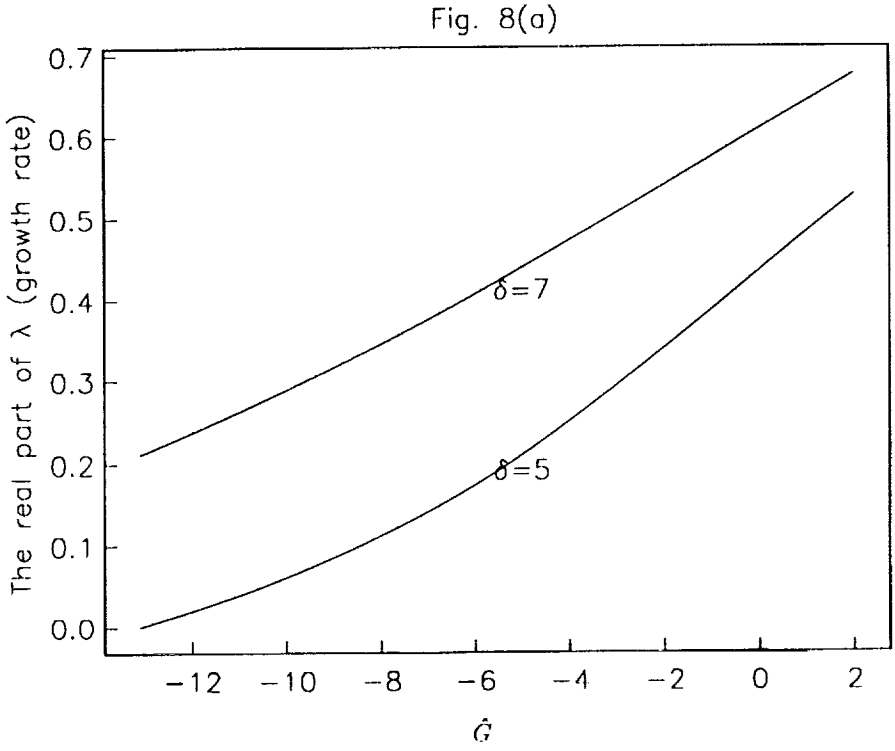

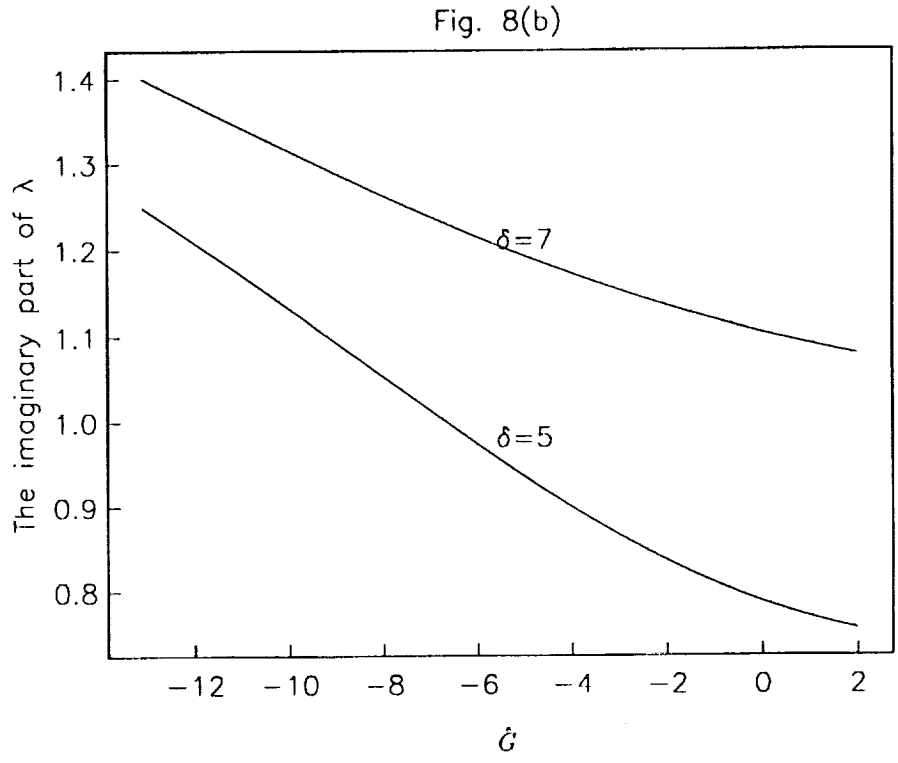

Figure 8. Dependence of (a) the growth rate and (b) the imaginary part of λ on $\hat{G}$ for $k = 0.1$ and $\delta = 5, 7$.

REPORT DOCUMENTATION PAGE

Form Approved
OMB No. 0704-0188

1. AGENCY USE ONLY (Leave blank)	2. REPORT DATE	3. REPORT TYPE AND DATES COVERED
	June 1992	Contractor Report

4. TITLE AND SUBTITLE
CROSSFLOW EFFECTS ON THE GROWTH RATE OF INVISCID GÖRTLER VORTICES IN A HYPERSONIC BOUNDARY LAYER

5. FUNDING NUMBERS
C NAS1-18605
WU 505-90-52-01

6. AUTHOR(S)
Yibin Fu
Philip Hall

7. PERFORMING ORGANIZATION NAME(S) AND ADDRESS(ES)
Institute for Computer Applications in Science and Engineering
Mail Stop 132C, NASA Langley Research Center
Hampton, VA 23665-5225

8. PERFORMING ORGANIZATION REPORT NUMBER
ICASE Report No. 92-26

9. SPONSORING/MONITORING AGENCY NAME(S) AND ADDRESS(ES)
National Aeronautics and Space Administration
Langley Research Center
Hampton, VA 23665-5225

10. SPONSORING/MONITORING AGENCY REPORT NUMBER
NASA CR-189667
ICASE Report No. 92-26

11. SUPPLEMENTARY NOTES
Langley Technical Monitor: Michael F. Card
Final Report
Submitted to Journal of Fluid Mechanics

12a. DISTRIBUTION/AVAILABILITY STATEMENT
Unclassified - Unlimited

Subject Category 34

12b. DISTRIBUTION CODE

13. ABSTRACT *(Maximum 200 words)*

The effects of crossflow on the growth rate of inviscid Görtler vortices in a hypersonic boundary layer with pressure gradient are studied in this paper. Attention is focused on the inviscid mode trapped in the temperature adjustment layer; this mode has greater growth rate than any other mode. The eigenvalue problem which governs the relationship between the growth rate, the crossflow amplitude and the wavenumber is solved numerically, and the results are then used to clarify the effects of crossflow on the growth rate of inviscid Görtler vortices. It is shown that crossflow effects on Görtler vortices are fundamentally different for incompressible and hypersonic flows. The neutral mode eigenvalue problem is found to have an exact solution, and as a by-product, we have also found the exact solution to a neutral mode eigenvalue problem which was formulated, but unsolved before, by Bassom and Hall (1991).

14. SUBJECT TERMS	15. NUMBER OF PAGES
boundary layer; instability; vortex	36
	16. PRICE CODE: A03

17. SECURITY CLASSIFICATION OF REPORT	18. SECURITY CLASSIFICATION OF THIS PAGE	19. SECURITY CLASSIFICATION OF ABSTRACT	20. LIMITATION OF ABSTRACT
Unclassified	Unclassified		

NSN 7540-01-280-5500

Standard Form 298 (Rev 2-89)
Prescribed by ANSI Std Z39-18
298-102

NASA-Langley, 1992